# Statistical model of particle emission from rapidly rotating spherical and deformed nuclei

V. P. Aleshin

*Institute of Nuclear Research, Ukrainian Academy of Sciences, Kiev*

Fiz. Elem. Chastits At. Yadra **21**, 963–999 (July–August 1990)

New results of the semiclassical theory of the statistical decay of spherical and deformed nuclei are presented systematically. Practical methods of calculating particle emission from ellipsoidal nuclei are described. Applications of the semiclassical approach to the description of the angular distributions of particles measured in coincidence with a $\gamma$-ray cascade, fission fragments, heavy ions, or other particles are considered.

## INTRODUCTION

The currently existing methods of statistical calculations can be divided into quantum (for example, Refs. 1–4) and semiclassical (Refs. 5–8) methods. The programs that realize these methods make it possible to follow one or several chains of decays, giving as a result the yield of isotopes, the number of emitted particles, and their energy spectra.

The programs of semiclassical type make it possible, in addition, to calculate the angular distributions and the angular correlations of different decay products. In principle, these quantities can also be calculated by means of the quantum formulas, but this requires much computer time and memory, particularly at large angular momenta.

Even greater difficulties for the quantum approach arise in the decay of strongly deformed systems. The interest in such systems is due to the fact that the experimental $\alpha$-particle yields are higher than what the calculations for spherical nuclei predict,[9] and the effective barriers deduced from the spectra of the emitted $\alpha$ particles are often lower than those obtained from reactions in which $\alpha$ particles fuse with the corresponding nucleus in the ground state.[10–14]

In Sec. 1 of this review we present a semiclassical statistical model of particle emission from spherical nuclei. In Sec. 2 we investigate the conditions for its applicability. In Sec. 3 we present a semiclassical statistical model for deformed nuclei. In Sec. 4 we give a practical realization of this model for ellipsoidal nuclei. In Sec. 5 we calculate correlation functions and compare them with experiment. We conclude with a summary.

## 1. SPHERICAL NUCLEI

### Decay probability

The point of departure for the semiclassical statistical theory of the decay of spherical nuclei[15–23] is an expression for the probability of decay (per unit time) of a nucleus with excitation energy $E$ and spin $\mathbf{I}$ associated with emission of a particle with energy $\varepsilon$ and orbital angular momentum $\mathbf{l}$ moving in the direction $\mathbf{n}$:

$$R(\varepsilon,\ \mathbf{l},\ \mathbf{n};\ E,\ \mathbf{I}) = \frac{g}{(2\pi)^3}\frac{\omega\left(E-S-\varepsilon-\frac{(\mathbf{I}-\mathbf{l})^2}{2J}\right)}{\omega_x(Q)}T_l(\varepsilon)\,\delta(\mathbf{ln}). \tag{1}$$

Here, $g$ is the number of spin substates of the particle, $S$ is the separation energy, $T_l(\varepsilon)$ is the transmission coefficient, $J$ is the moment of inertia of the daughter nucleus, $\omega = (2j+1)^{-1}\rho$ and $\omega_x = (2I+1)^{-1}\rho_x$ are the reduced level densities of the daughter and parent nuclei, $Q$ is the difference between the excitation energy and rotational energy of the parent nucleus, and $\hbar = 1$.

The distribution (1) gives the most complete description of the decay, since from given $\varepsilon$, $E$, $\mathbf{l}$, $\mathbf{I}$, and $\mathbf{n}$ it is possible to calculate the excitation energy $u$, the angular momentum $\mathbf{j}$, and the momentum of the recoil nucleus and, therefore, the probabilities of its subsequent transformations.

If the width of the energy spectrum of the emitted particles is small compared with the thermal energy $q = u - j^2/(2J)$ of the daughter nucleus, then for $\omega(q)$ one can use the thermal approximation

$$\omega(q) = \omega(q')\exp[(q-q')/\tau], \tag{2}$$

where the temperature $\tau$ is expressed in terms of $q'$ in the form

$$\tau = [d\ln\omega(q)/dq]^{-1}_{q=q'}. \tag{3}$$

The function $\omega(q)$ is often parametrized in the form proposed by Lang.[24] In this case, apart from a constant factor we have

$$\omega(q) = \exp[2(a(q-\Delta))^{1/2}]/[t^4(Ja)^{3/2}], \tag{4}$$

where

$$t = \frac{3}{4a} + \left(\left(\frac{3}{4a}\right)^2 + \frac{q-\Delta}{a}\right)^{1/2}.$$

The level-density parameter is $a = A/8\ \mathrm{MeV}^{-1}$ for $A < 100$ and $A/12\ \mathrm{MeV}^{-1}$ for $A > 100$ (Refs. 25 and 26), and the correction for pairing is $\Delta = 1.2$ MeV for odd nuclei, $\Delta = 2.4$ MeV for even–even nuclei, and $\Delta = 0$ for odd–odd nuclei. For $J$ the rigid-body expression with $r_0 = 1.2$ fm is used.

For $\omega(q)$ as defined in (4) the relation (3) takes the form

$$\tau = \frac{2}{a} + \left(\left(\frac{2}{a}\right)^2 + \frac{q'-\Delta}{a}\right)^{1/2}. \tag{5}$$

If for $\omega(q)$ we use (2), and for $T_l(\varepsilon)$ the classical model, then the expression (1) simplifies to the form

$$R = C\ \exp\left(-\frac{\varepsilon}{\tau} + \frac{\omega\mathbf{l}}{\tau} - \frac{l^2}{2J\tau}\right)\Theta\left(\varepsilon - E_0 - \frac{l^2}{2mR_0^2}\right)\delta(\mathbf{nl}), \tag{6}$$

where

$$C = \frac{g}{(2\pi)^3}\exp\left[\left(E-S-\frac{I^2}{2J}-q'\right)\Big/\tau\right]\omega(q')/\omega_x(Q);$$

$\omega = \mathbf{I}/J$ is the rotation frequency; $\theta(x)$ is the step function;

 0090-4759/90/040407-17$04.00  

$E_0$ and $R_0$ are the height and radius of the barrier; and $m$ is the particle mass.

The height of the barrier is often taken in the form

$$E_0 = Z_p Z_d e^2/R_e,$$

where

$$R_e = \begin{cases} [2{,}452 - 0{,}408 \log_{10}(Z_p Z_d)]\, A_d^{1/3} + 2{,}53 & \text{for } \alpha, \\ 1{,}81\, A_d^{1/3} + 1{,}44 & \text{for } p, \end{cases} \quad (7)$$

while for the barrier radius the following values are taken:

$$R_0 = [2{,}0337 - 0{,}2412 \log_{10}(Z_p Z_d)]\, A_d^{1/3} + \begin{cases} 2{,}53 & \text{for } \alpha, \\ 1{,}44 & \text{for } p, \end{cases} \quad (8)$$

where $Z_p$, $Z_d$ and $A_p$, $A_d$ are the charge and mass numbers of the emitted particle and the daughter nucleus, respectively; $R_e$ and $R_0$ are given in fermis. The expressions (7) and (8) were obtained in Ref. 27 as a result of systematization of the cross sections for absorption of protons and $\alpha$ particles by medium and heavy nuclei. If $q'$ is identified with the mean $q$ found by means of the distribution (6) and the result is substituted in the right-hand side of (5), we obtain an equation for $\tau$, and by solving it we obtain values for all the parameters that occur in (6).

#### The coefficients $T_l(\varepsilon)$

Using the distribution $R$, we can calculate the emission widths, the mean values of $\varepsilon$, $l$, $j$, the energy and angular distributions of the particles, and the two-particle correlations. Among these quantities there are some for which an integration over $d\varepsilon$ is performed when they are obtained. A feature of these quantities is that for their calculation one needs, not the $T_l(\varepsilon)$ themselves, but the corresponding Laplace transform ($s = \tau^{-1}$):

$$L_l(s) = \int_0^\infty d\varepsilon \exp(-s\varepsilon)\, T_l(\varepsilon). \quad (9)$$

It was shown in Refs. 11, 25, 26, and 28–34 that when the classical $T_l(\varepsilon)$ are used simple analytic expressions are obtained for quantities of the indicated type. This possibility is explained by the fact that for the classical $T_l$ the Laplace transform has a very simple form,

$$L_l(s) = s^{-1} \exp\left\{-\left[E_0 + \frac{l^2}{2mR_0^2}\right] s\right\}, \quad (10)$$

as a result of which the integration in the corresponding expressions over the variables in the set $l$, $\mathbf{l}$, $\mathbf{n}$, $j$ can be performed explicitly.

Unfortunately, the use of an abrupt step for $T_l(\varepsilon)$ is not always justified, particularly for neutrons. In addition, it is difficult to compare calculations with such $T_l(\varepsilon)$ with the quantum calculation, since the connection between $E_0$ and $R_0$ and the optical coefficients $T_l(\varepsilon)$ is unknown.

Calculations show that for $\tau > 1$ MeV the expression (10) gives a good approximation of $L_l(s)$ with the optical $T_l(\varepsilon)$ if $E_0$ and $1/R_0^2$ are regarded as linear functions of $s$. Thus, we arrive at the parametrization

$$L_l(s) = s^{-1} \exp\{-[(b_0 - b_1 s) + (c_0 - c_1 s)\, l^2]\, s\}. \quad (11)$$

In what follows, it will be seen that the use of (11) instead of (10) only slightly complicates the analytic expressions for the quantities mentioned at the beginning of this subsection. The constants $b_0$, $b_1$, $c_0$, and $c_1$ can be regarded as phenomenological parameters, or they can be found by means of a linear approximation with respect to $l^2$ and $s$ for the functions $s^{-1}\ln[sL_l(s)]$, calculated with the optical $T_l(\varepsilon)$.

Substituting (9) into the left-hand side of (11), we obtain an integral equation for $T_l(\varepsilon)$. Assuming that this equation is valid for all $s > 0$ and shifting the lower limit of the integral over $d\varepsilon$ to $-\infty$, we can solve the equation for $T_l(\varepsilon)$ analytically. The result has the form

$$T_l^{\mathrm{erf}}(\varepsilon) = \frac{1}{2}\left[1 + \mathrm{erf}\left(\frac{\varepsilon - \varepsilon_l}{D_l 2^{1/2}}\right)\right], \quad (12)$$

where $\mathrm{erf}(x)$ is the error function, and $\varepsilon_l$ and $D_l$, which determine the position and width of the smooth step function, are given by

$$\varepsilon_l = b_0 + c_0 l^2, \quad D_l^2 = 2(b_1 + c_1 l^2). \quad (13)$$

The relation (12) is analogous to the Hill–Wheeler formula[35] for the transmission coefficient. This analogy can be used to estimate the parameters $b_0$, $b_1$, $c_0$, and $c_1$. To this end, we rewrite $T_l^{\mathrm{erf}}(\varepsilon)$ in the form

$$T_l^{\mathrm{erf}}(\varepsilon) = \int_{-\infty}^{\infty} dX\, \frac{\exp(-X^2/(2D_l^2))}{(2\pi)^{1/2} D_l}\, \Theta(\varepsilon - (b_0 + X) - c_0 l^2). \quad (14)$$

This relation shows that the diffused transmission coefficients can be obtained by averaging the classical $T_l(\varepsilon)$ over the barrier height.

The Hill–Wheeler coefficients can be represented in a form analogous to (14) if the Gaussian on the right-hand side of (14) is replaced by the function

$$w^{\mathrm{HW}}(X) = (2\hbar\omega_l/\pi)\, \mathrm{ch}^{-2}\left(\frac{\pi X}{\hbar\omega_l}\right)$$

and the substitutions $b_0 = E_0$ and $c_0 = (2mR_0^2)^{-1}$ are made. The parameter $D_l$ can be identified with the standard deviation for the distribution $w^{\mathrm{HW}}(X)$, which is equal to $\hbar\omega_l/(2\sqrt{3})$. Bearing in mind that for protons and $\alpha$ particles $\hbar\omega_0 = 3.8$ MeV (Ref. 27), we find that for these particles $D_0 = 1.1$ MeV.

#### Distributions with respect to $\varepsilon$, l, j

The key quantity in the quantum statistical model of decay is the probability $R(\varepsilon, l, j; E, I)$ of the decay per unit time of nucleus $E$, $I$ into particle $\varepsilon$, $l$ and residual nucleus $j$. Taking $\mathbf{I}$ as the polar axis, denoting by $\beta_l$ and $\gamma_l$ the polar and azimuthal angles of the orientation of $\mathbf{l}$, and going over from $\beta_l$ to $j$ by means of the formula

$$\cos\beta_l = (I^2 + l^2 - j^2)/(2Il),$$

we can represent the corresponding classical probability in the form[17]

$$R(\varepsilon, l, j; E, I) = \int R(\varepsilon, \mathbf{l}, \mathbf{n}; E, \mathbf{I})\, d\mathbf{n} l^2\, [d\cos\beta_l/dj]\, d\gamma_l. \quad (15)$$

The normalized distribution with respect to $\varepsilon$, $l$, $j$ has

the form

$$P(\varepsilon,\ l,\ j;\ E,\ I)=\frac{R(\varepsilon,\ l,\ j;\ E,\ I)}{R(E,\ I)}, \tag{16}$$

where

$$R(E,\ I)=\int R(\varepsilon,\ l,\ j;\ E,\ I)\,d\varepsilon\,dl\,dj \tag{17}$$

is the total probability of emission of a particle per unit time. By means of $P(\varepsilon, l, j; E, I)$ for fixed $E, I$ we can calculate the mean value of an arbitrary function $f(\varepsilon, l, j)$ of the quantities $\varepsilon, l, j$. Denoting such averaging by a bar, we have

$$\overline{f}=\int d\varepsilon\,dl\,djf(\varepsilon,\ l,\ j)\,P(\varepsilon,\ l,\ j;\ E,\ I). \tag{18}$$

The expressions (2) for $\omega(q)$ and (9) and (11) for $T_l(\varepsilon)$ enable us to calculate (15), (16), (17), and also the mean values of $\varepsilon, l^2, j^2$, analytically. The total probability of particle emission per unit time, (17), takes the form

$$R(E,\ I)=\frac{g}{\pi}\frac{\omega(q')}{\omega_x(Q)}\frac{\tau^2}{p}J\beta_c \times\exp\left[\left(E-S-b_0+\frac{b_1}{\tau}-\frac{I^2}{2J}-q'\right)\Big/\tau\right]. \tag{19}$$

Here

$$p=\frac{2}{\pi^{1/2}}\frac{x\exp(-x^2)}{\operatorname{erf}(x)},\quad x=I\left(\frac{\beta_c}{2J\tau}\right)^{1/2},\qquad \beta_c=\frac{J_c}{J+J_c},\quad J_c=\frac{1}{2}\frac{1}{c_0-c_1/\tau}. \tag{20}$$

With allowance for (2), (9), (11), and (19), the weight function (16) can be represented in the form

$$P(\varepsilon,\ l,\ j;\ E,\ I)=\frac{pj}{2J\tau^2I\beta_c}\varepsilon_{ljI}T_l(\varepsilon) \times\exp\left[-\left(\varepsilon+\frac{j^2}{2J}-\frac{I^2}{2J}\right)\Big/\tau\right], \tag{21}$$

where $\varepsilon_{ljI}=1$ if $l, j$, and $I$ can form a triangle, and $\varepsilon_{ljI}=0$ otherwise.

Using (18) and (21), we find the mean values

$$\overline{\varepsilon}=b_0-\frac{2b_1}{\tau}+\tau+\frac{1}{2}\left[\frac{\beta_c^2I^2}{J_c}+\tau(1-\beta_c)(1+p)\right] \times\left(1-\frac{c_1}{c_0\tau-c_1}\right); \tag{22}$$

$$\overline{j^2}=(1-\beta_c)^2I^2+2J\tau\left[\frac{1}{2}\beta_c+1+\left(\frac{1}{2}\beta_c-1\right)p\right]; \tag{23}$$

$$\overline{l^2}=\beta_c^2I^2+\tau J\beta_c(1+p). \tag{24}$$

The expressions (19) and (21)–(24) contain the parameter $\tau$, the numerical value of which is not determined until $q'$ on the right-hand side of (5) is determined. In what follows, we shall identify $q'$ with the mean thermal energy of the daughter nucleus:

$$\overline{q}=E-S-\overline{\varepsilon}-\frac{\overline{j^2}}{2J}. \tag{25}$$

The relations (22), (23), and (25) enable us to find the dependence of $\overline{q}$ on $\tau$. Substituting this dependence on the right-hand side of (5) in place of $q'$, we obtain a closed equation for $\tau$.

If $\tau$ satisfies the conditions

$$c_0\gg\frac{c_1}{\tau},\ b_0\gg\frac{b_1}{\tau},\ I\left(\frac{\beta_c}{2J\tau}\right)^{1/2}\ll 1,$$

then in the equation for $\tau$ the terms containing $c_1$ and $b_1$ can be omitted and we can set $p=1$. The equation then obtained can be solved explicitly. Its root

$$\tau_0=a^{-1}+\sqrt{a^{-2}+a^{-1}\left(E-S-b_0-\Delta-\frac{I^2}{2J+c_0^{-1}}\right)}$$

can be used as a first approximation in a search for $\tau$ by the method of iteration. For this, using $\tau_0$, we calculate $\overline{\varepsilon_0}$ and $\overline{j_0^2}$ in accordance with (22) and (23), and then also $\overline{q_0}$ using (25). Substituting this $\overline{q_0}$ into the right-hand side of (5), we obtain $\tau_1$, after which the procedure is repeated.

### Angular distributions and correlations

The probability of emission of a particle in the direction $\mathbf{n}$ from the nucleus $(E, \mathbf{I})$ has the form

$$W(\mathbf{n};\ E,\ \mathbf{I})=\frac{R(\mathbf{n};\ E,\ \mathbf{I})}{R_{\text{tot}}(E,\ I)},$$

where the distribution function $R(\mathbf{n}; E, \mathbf{I})$ is obtained by integrating (1) over $d\varepsilon d^3l$, and $R_{\text{tot}}(E, I)$ is the sum of the $R(E, I)$ determined in (19) from the various emitted particles. Integrating over $d^3l$ in Cartesian coordinates with the $z$ axis directed along $\mathbf{n}$, we obtain

$$W(\mathbf{n};\ E,\ \mathbf{I})=G\exp\left[-\alpha(\mathbf{In})^2\right], \tag{26}$$

where

$$G=\frac{1}{4\pi}\frac{R(E,\ I)}{R_{\text{tot}}(E,\ I)}\frac{\alpha^{1/2}I}{\operatorname{Erf}(\alpha^{1/2}I)},\quad \alpha=\frac{\beta_c}{2J\tau}, \tag{27}$$

and the error function

$$\operatorname{Erf}(x)=\frac{\pi^{1/2}}{2}\operatorname{erf}(x)$$

is normalized by the condition $\operatorname{Erf}(x)/x\to 1$ as $x\to 0$.

The ratio

$$P(\varepsilon,\ \mathbf{l};\ \mathbf{n},\ E,\ \mathbf{I})=\frac{R(\varepsilon,\ \mathbf{l},\ \mathbf{n};\ E,\ \mathbf{I})}{R(\mathbf{n};\ E,\ \mathbf{I})}$$

can be used as a normalized distribution of $\varepsilon$ and $l$ for fixed values of $\mathbf{n}, E$, and $\mathbf{I}$. Denoting the averaging by means of the distribution $P(\varepsilon, \mathbf{l}, \mathbf{n}, E, \mathbf{I})$ by angular brackets, we find

$$\langle\varepsilon\rangle=b_0-\frac{b_1}{\tau}+\left(1+\frac{J}{J+J_c}\right)\tau+\frac{J_c}{2(J+J_c)^2}[\mathbf{I}\times\mathbf{n}]^2, \tag{28}$$

$$\langle\mathbf{l}\rangle=\beta_c[\mathbf{I}-\mathbf{n}(\mathbf{In})]. \tag{29}$$

We now consider the successive emission of two particles in the directions $\mathbf{n}_1$ and $\mathbf{n}_2$ from the compound nucleus $E, \mathbf{I}$. We obtain the probability of the first decay from (26) and (27) by appending the index 1 to the quantities that characterize the decay products. We obtain the probability of the second decay from (26) and (27) by appending the index 2 to the quantities that characterize the decay products and by replacing $E, I$, and $\mathbf{I}$ by

$$u_1=E-S_1-\overline{\varepsilon}_1,\quad I_1=(\overline{j_1^2})^{1/2},\ \text{and}\ \mathbf{I}_1=\mathbf{I}-\langle\mathbf{l}_1\rangle,$$

respectively, where $\varepsilon_1$, $\overline{j_1^2}$, and $\langle\mathbf{l}_1\rangle$ are obtained from (22), (23), and (29) by appending to the quantities that characterize the decay products the index 1. The probability of the complete process, $W(\mathbf{n}_1, \mathbf{n}_2; E, \mathbf{I})$, is the product of the two single-particle probabilities and can be represented in the form

$$W(\mathbf{n}_1, \mathbf{n}_2; E, \mathbf{I}) = G_{12} \exp[-B(\mathbf{In}_1)^2 - C(\mathbf{In}_2)^2 - D(\mathbf{In}_1)(\mathbf{In}_2)(\mathbf{n}_1\mathbf{n}_2)], \quad (30)$$

where

$$G_{12} = G_1 G_2,\ B = \alpha_1,\ C = \alpha_2 - D,\ D = 2\alpha_2\beta_{c1}. \quad (31)$$

The first and second terms in the exponential in Eq. (30) characterize the correlation of $\mathbf{n}_1$ and $\mathbf{n}_2$ with $\mathbf{I}$. The correlation between $\mathbf{n}_1$ and $\mathbf{n}_2$ is contained in the last term. In a large system $\beta_{c1} \to 0$, and the contribution of this term will be negligibly small compared with the contribution of the first two terms.

By means of (30) it is easy to construct the angular correlation function for two particles emitted from a compound nucleus formed in a fusion reaction. Taking the $z$ axis along the beam, placing the $x$ axis in the plane formed by $\mathbf{n}_1$ and $\mathbf{n}_2$, and directing it in such a way that the component of $\mathbf{n}_1$ along the $x$ axis is positive, we obtain

$$W(\mathbf{n}_1, \mathbf{n}_2) = \int_0^{I_{\max}} I\,dI \int_0^{2\pi} d\Phi W(\mathbf{n}_1, \mathbf{n}_2; E, \mathbf{I}_\Phi), \quad (32)$$

where $\mathbf{I}_{\max}$ is the maximal spin for a spin distribution in the form of a triangle; $\mathbf{I}_\Phi$ is a vector of length $I$ situated in the plane $xOy$ and making angle $\Phi$ with the $x$ axis.

Substituting (30) in (32) and integrating over $d\Phi$, we obtain[31-33]

$$W(\theta_1, \theta_2, \phi) = \int_0^{I_{\max}} I\,dI\,G_{12} \exp\left(-\frac{1}{2}HI^2\right) \times I_0\left[\frac{1}{2}(H^2+M)^{1/2}I^2\right], \quad (33)$$

where $I_0(x)$ is the modified Bessel function of zeroth order;

$$H = B\sin^2\theta_1 + C\sin^2\theta_2 + D\cos\theta_{12}\sin\theta_1\sin\theta_2\cos\phi;$$
$$M = (D^2\cos^2\theta_{12} - 4BC)\sin^2\theta_1\sin^2\theta_2\sin^2\phi; \quad (34)$$

$\theta_1$ and $\theta_2$ are the polar angles of the vectors $\mathbf{n}_1$ and $\mathbf{n}_2$, respectively; $\theta_{12}$ is the angle between these vectors; and $\phi = \phi_1 - \phi_2$ is the difference between the azimuthal angles $\mathbf{n}_1$ and $\mathbf{n}_2$. If particles 1 and 2 are identical, then Eq. (33) is the final equation. Otherwise, it must include an additional term in which the order of emission is reversed.

## 2. COMPARISON WITH QUANTUM CALCULATIONS

### Connection between the classical and quantum approaches

The quantum expression for the double differential cross section for emission of a particle by a compound nucleus formed in a fusion reaction has the form

$$\frac{d^2\sigma}{d\mathbf{n}\,d\varepsilon} = \sum_I \sigma(E, I)\frac{R(\varepsilon, \mathbf{n}; E, I)}{R_{\text{tot}}(E, I)}, \quad (35)$$

where $\sigma(E, I) = \pi\lambda^2(2I+1)T_I(E_i)$ is the cross section for the production of the compound nucleus $(E, I)$; $\lambda$ and $T_I(E_i)$ are the wavelength and transmission coefficient in the entrance channel; and

$$R(\varepsilon, \mathbf{n}; E, I) = \sum_{j\mu lm} |Y_{lm}(\mathbf{n})|^2 |C^{I0}_{j\mu lm}|^2 R(\varepsilon, l, j; E, I) \quad (36)$$

is the probability of decay per unit time with emission of the particle $(\varepsilon, \mathbf{n})$. The summation is over the quantum numbers of the spin of the residual nucleus, $j, \mu$, and the orbital angular momentum of the particle, $l, m$. The $z$ axis is taken along the direction of the beam, and

$$R(\varepsilon, l, j; E, I) = \varepsilon_{ljI}\frac{g}{2\pi}T_l(\varepsilon)\frac{\rho(E-S-\varepsilon, j)}{\rho_x(E, I)}. \quad (37)$$

To deduce the key relation (1) of the semiclassical model from the quantum expressions (36) and (37), we replace the Clebsch–Gordan coefficients $C^{I0}_{j\mu lm}$ and the spherical functions $Y_{lm}(\mathbf{n}) = ((2l+1)/4\pi)^{1/2}D^l_{m0}(\mathbf{n})$ by the semiclassical expressions in the form of the integrals

$$|C^{IM}_{j\mu lm}|^2 = \frac{I^2 jl}{4\pi^2}\int d\Omega_I\,d\Omega_j\,d\Omega_l\,\delta(\mathbf{I}-\mathbf{j}-\mathbf{l})\,\delta(M - I\cos\theta_I) \times \delta(\mu - j\cos\theta_j)\,\delta(m - l\cos\theta_l); \quad (38)$$

$$|D^l_{mk}(\mathbf{n})|^2 = \frac{l}{2\pi}\int d\Omega_l\,\delta(l\cos\theta_l - m)\,\delta(\mathbf{ln} - k), \quad (39)$$

where $d\Omega_I$, $d\Omega_j$, $d\Omega_l$ are the infinitesimal solid angles, and $\theta_I$, $\theta_j$, $\theta_l$ are the polar angles of the vectors $\mathbf{I}, \mathbf{j}, \mathbf{l}$, respectively. The expressions (38) and (39) have a transparent physical interpretation, and after the integrals over the angles have been calculated they lead to the standard classical representations first obtained in Ref. 36.

Substituting (37)–(39) in (36), replacing the sums over $j, \mu, l, m$ by integrals, integrating over $dm\,d\mu\,d\theta_l\,d\theta\,dd_j^3$, denoting the azimuthal angles of the vectors $\mathbf{l}, \mathbf{n}, \mathbf{I}$ by $\phi_l, \phi_n, \Phi_I$, respectively, and using the identity

$$\int \delta(\mathbf{ln})\,d\phi_l = \int \delta(\mathbf{ln})\,d\phi_n,$$

we arrive at the relation

$$R(\varepsilon, \mathbf{n}; E, I) = \int\frac{d\phi_n}{2\pi}\int\frac{d\Phi_I}{2\pi}\int d^3l \times \frac{g}{(2\pi)^3}\frac{\omega\left(E-S-\varepsilon-\frac{(\mathbf{I}-\mathbf{l})^2}{2J}\right)}{\omega_x(Q)}T_l(\varepsilon)\,\delta(\mathbf{ln}).$$

In the integrand of this expression we readily recognize the classical decay probability $R(\varepsilon, \mathbf{l}, \mathbf{n}; E, \mathbf{I})$ defined in (1). Note that after integration over $d^3l$ and averaging over $d\Phi_I$ the result will not depend on $\phi_n$. Therefore, the averaging over $d\phi_n$ can be removed.

### Criterion for applicability

We shall discuss the conditions for applicability of the semiclassical approximation for the example of the angular distribution of particles with fixed $\varepsilon$ and $l$ emitted by a nucleus with given $\mathbf{I}$. In accordance with (6), in the classical case this distribution is proportional to the integral

$$W_c(\beta) = \frac{l}{2\pi}\int d\Omega_l \exp\left(\frac{\omega\mathbf{l}}{\tau}\right)\delta(\mathbf{ln}),$$

where $\beta$ is the angle between $\mathbf{n}$ and $\mathbf{I}$. Using (39), we can readily verify that the quantum analog of this integral is the sum

$$W_q(\beta) = \sum_m e^{\lambda m}|D^l_{m0}(\mathbf{n})|^2,$$

where $\lambda = \omega/\tau$.

Comparison of $W_c(\beta)$ with $W_q(\beta)$ is facilitated by the fact that both distributions can be calculated analytically, leading to the modified Bessel function $I_0[(l+\frac{1}{2})\lambda\sin\beta]$

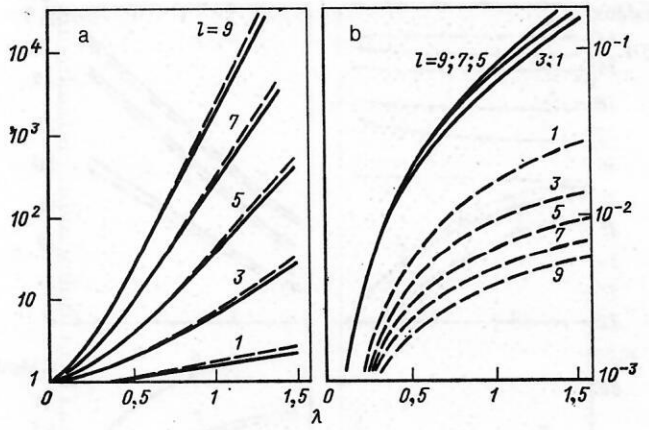


FIG. 1. Comparison of calculated values of the angular anisotropy as a function of $\lambda$ for different $l$: a) quantum calculation, $A_q$ (continuous curves), and classical calculation, $A_c$ (broken curves); b) relative errors $(A_c - A_q)/A_q$ (continuous curves) and $|A_q - \tilde{A}_c|/A_q$ (broken curves); the continuous curves for $l = 9, 7, 5$ cannot be distinguished.

(Ref. 16) and the Legendre polynomial $P_l[1 + (\cosh\lambda - 1)\sin^2\beta]$ (Ref. 37), respectively. Since these functions are symmetric with respect to 90° and increase monotonically in the interval 0–90°, it is sufficient to compare the corresponding anisotropies:

$$A_c = W_c(90°)/W_c(0°) = I_0\left[\left(l+\frac{1}{2}\right)\lambda\right],$$
$$A_q = W_q(90°)/W_q(0°) = P_l(\mathrm{ch}\,\lambda).$$

This is done in Fig. 1.

Since $A_q$ and $A_c$ increase very rapidly with increasing $\lambda$ and $l$, we plot them on a logarithmic scale (see Fig. 1a). However, the difference between $A_c$ and $A_q$ is then almost indistinguishable. Therefore, we show separately (in Fig. 1b) the relative error $r = |A_c - A_q|A_q$. It can be seen that for the $l$ of practical interest ($l < 10$), the value of $r$ does not exceed a few percent for $\lambda < 1$. Thus, the criterion for applicability of the semiclassical approximation is the inequality $\hbar\omega/\tau < 1$, in which we have restored Planck's constant.

If, for fixed $\lambda$, $r$ were to tend to zero as $l \to \infty$, then $A_c$ would be an asymptotic approximation for $A_q$. It can be seen from Fig. 1 that this is not the case, since for given $\lambda$ the value of $r$ increases with $l$, though admittedly very slowly. It can be seen from Fig. 1 that an asymptotic approximation for $A_q$ is provided by the function $\tilde{A}_c = (\lambda/\sinh\lambda)^{1/2}A_c$, which we have introduced by analogy with the asymptotic approximation for the Legendre polynomial in terms of a Bessel function,

$$P_l(\cos\chi) = (\chi/\sin\chi)^{1/2}J_0\left[\left(l+\frac{1}{2}\right)\chi\right],$$

which is given, for example, in Ref. 38.

This example leads to the following observation. Although the expression (39) for $|D^l_{mk}(\mathbf{n})|^2$ is in itself very crude (it does not take into account the oscillations and describes only the envelope), if both sides of (39) are multiplied by a bell-shaped function of $m$ (with a width of a few units) and we sum over $m$ on the left and integrate on the right, we arrive at an equation that holds to very good accuracy.

This property is quite generally characteristic of the comparison of the quantum and classical distributions. As a further example we give the relation

$$\sum_{j\mu}(2j+1)\exp[-\gamma j(j+1)]|C^{IM}_{j\mu lm}|^2$$
$$= (2I+1)\exp[-\gamma(I^2+l^2-2Mm)]$$
$$\times I_0[2\gamma\sqrt{(I^2-M^2)(l^2-m^2)}],$$

which is readily proved by means of (38). If we substitute $\gamma = (2J\tau)^{-1}$, $M = 0$. Fix $I$ and $l$ and regard $m$ as a variable, then the resulting relation will be more accurate, the better is the fulfillment of the inequality $\hbar\omega'/\tau < 1$, where $\omega' = (I-l)/J$ differs somewhat from the $\omega = I/J$ introduced earlier. This is demonstrated by the calculations made in Ref. 39.

### Accuracy of approximations for $\omega(q)$ and $L_l(s)$

To obtain an idea of the errors introduced by the thermal approximation for $\omega(q)$ and by the approximation (11) for $L_l(s)$, we consider the decay of $^{74}$Kr formed by fusion of $^{16}$O with $^{58}$Ni at laboratory energy 70 MeV, corresponding to an excitation energy of the $^{74}$Kr compound nucleus of $E = 51.9$ MeV (Ref. 28). In the calculations, we take into account the emission of neutrons, protons, and $\alpha$ particles.

The quantum calculations were made using the program GROGI (Refs. 1 and 2) with the optical-model parameters given in Table I.

The values of $b_0$, $b_1$, $c_0$, $c_1$ obtained by fitting $L_l(s)$ to the optical $T_l(\varepsilon)$ by means of (11) are given in Table II. Table III gives the reduced radii of the Coulomb barrier in the $p$ and $\alpha$ decay channels at several temperatures, calculated by means of the relation

$$r_{0,c} = \frac{Z_pZ_de^2}{(A_p^{1/3}+A_d^{1/3})\left(b_0-\frac{b_1}{\tau}\right)}.$$

It is readily seen that $r_{0,c}$ at lower $r$ exceeds the reduced radii

$$r_0' = \frac{R_e}{A_p^{1/3}+A_d^{1/3}}$$

calculated for the $R_e$ determined in (7).

In Fig. 2 we have plotted as functions of $I$ the following quantities: the mean excitation energy $\bar{u}$, the angular mo-

TABLE I. Optical-model parameters in the program GROGI.

| Channel | $V$, MeV | $r_V$, fm | $a_V$, fm | $W$, MeV | $r_W$, fm | $a_W$, fm | $V_{so}$, MeV | $r_{so}$, fm | $a_{so}$, fm | $r_c$, fm |
|---|---|---|---|---|---|---|---|---|---|---|
| $n$ | 48 | 1,17 | 0,75 | 10,8 | 1,27 | 0,60 | 6,2 | 1,01 | 0,75 | — |
| $p$ | 49 | 1,17 | 0,75 | 10,8 | 1,32 | 0,51 | 6,2 | 1,01 | 0,75 | 1,25 |
| $\alpha$ | 180 | 1,20 | 0,75 | 15,0 | 1,70 | 0,60 | — | — | — | 1,30 |

TABLE II. Penetrability parameters $T_l^{\text{erf}}(\varepsilon)$ for decay of $^{74}$Kr.

| Channel | $b_0$, MeV | $b_1$, MeV$^2$ | $c_0$, MeV | $c_1$, MeV$^2$ |
|---|---|---|---|---|
| $n$ | 0,856 | 0,162 | 0,340 | 0,091 |
| $p$ | 6,709 | 1,005 | 0,363 | 0,109 |
| $\alpha$ | 10,348 | 0,736 | 0,075 | 0,016 |

mentum $\tilde{j} = (\overline{j^2})^{1/2}$, and the branching ratio

$$K = R(E, I)/R_{\text{tot}}(E, I)$$

for $n$, $p$, and $\alpha$ calculated in accordance with the quantum and classical formulas, and also the temperature $\tau$ of the daughter nuclei. It can be seen that the semiclassical calculations with the thermal approximation for $\omega(q)$ and the approximation (11) for $L_l(s)$ agree very well with the quantum calculations made without these approximations.

The figure shows that with increasing $I$ the fraction of emitted $\alpha$ particles increases. The reason for this is that after emission of an $\alpha$ particle the nucleus has less spin than after emission of an $n$ or $p$. And since $\omega(q)$ increases with decreasing $j$, the emission of an $\alpha$ is more probable. The decrease of $\tau$ with increasing $I$ is due to the decrease of the thermal energy on account of the increase in the rotational energy.

The chain curve in Fig. 2 shows the calculation with $b_1 = c_1 = 0$, i.e., for $T_l(\varepsilon)$ in the form of an abrupt step. It can be seen that $\tilde{j}$ is hardly changed, but that $K$ and, especially, $\bar{u}$ have changed appreciably. Thus, $\bar{u}$ in the $p$ channel has become smaller by 1–1.2 MeV and, therefore, the mean kinetic energy of the protons has increased by the same amount.

### Other approximations

The more consistent derivation of the expressions (33) and (34) for the two-particle correlation function made in Ref. 31 shows that they are based on the following assumptions: 1) neglect of the terms proportional to $\beta_c^2$ in the exponential of (30); 2) replacement of the mean of the function of $\varepsilon$ and $\mathbf{j}$ by the function of the mean values of these quantities; 3) the use of $\bar{\varepsilon}$ in place of $\langle\varepsilon\rangle$ in the calculation of $G_2$.

These simplifications are evidently justified when $(\tilde{l}/I)^2 \ll 1$. To verify this assumption, we consider the angular correlations $W(\phi)$ for the reaction $^{58}$Ni($^{16}$O, $\alpha\alpha$) at $E_{\text{lab}} = 70$ MeV and $\theta_1 = \theta_2 = 110°$ in the center-of-mass system.[28] The first stage of this reaction has been described above. The measured and calculated $W(\phi)$ are shown in Fig. 3. As was expected, the agreement between the simplified semiclassical calculations and the quantum curves obtained

TABLE III. Reduced radius of Coulomb barrier, $r_0$, $c$, fm, for different $\tau$.

| Channel | $\tau = 0{,}5$ MeV | $\tau = 1$ MeV | $\tau = \infty$ |
|---|---|---|---|
| $p$ | 2,07 | 1,71 | 1,45 |
| $\alpha$ | 1,93 | 1,78 | 1,66 |

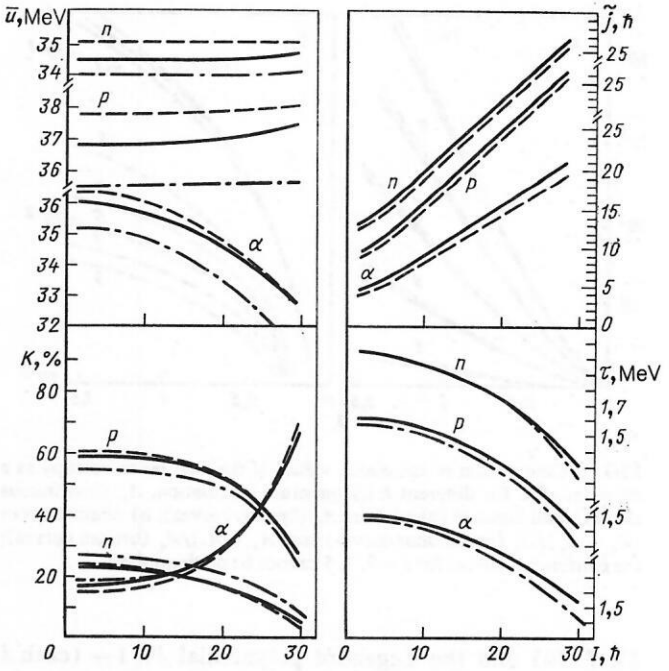


FIG. 2. Dependence of $\bar{u}, \tilde{j}, K$, and $\tau$ on $I$ for emission of $n, p$, and $\alpha$ from $^{74}$Kr with $E = 51.9$ MeV: the broken curves represent the quantum calculation; the continuous curves, the semiclassical calculation; and the chain curves, the semiclassical calculation with $b_1 = c_1 = 0$.

in Ref. 28 improves with increasing $I_{\max}$. At $I_{\max} = 32$, the results of the two calculations are almost identical and are close to the experimental points.

If in (31) we set $D = 0$, then in the corresponding correlation function (we denote it by $W_0$) the distortion of the spin distribution of the nucleus by the emission of the first particle will not be taken into account. It can be seen from Fig. 3 that $W_0$ has a greater anisotropy than $W$. As calculations show, to make $W_0$ and $W$ agree it is necessary to reduce $I_{\max}$ by half the mean orbital angular momentum of the $\alpha$ particle.

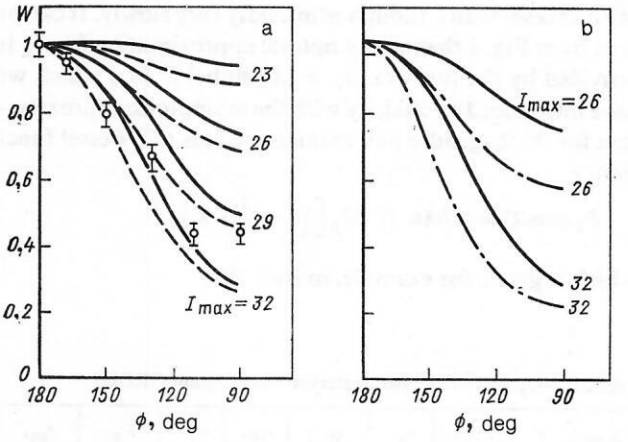


FIG. 3. Angular correlations of the two $\alpha$ particles from the $^{58}$Ni($^{16}$O, $\alpha\alpha$) reaction at $E_{\text{lab}} = 70$ MeV, $\theta_1 = \theta_2 = 110°$: a) comparison of the experiment (open circles) with quantum (broken curves) and semiclassical (continuous curves) calculations; b) comparison of semiclassical calculations for $D \neq 0$ (continuous curves) and $D = 0$ (chain curves).

## 3. DEFORMED NUCLEI

### Decay probability

In this subsection we derive an expression for the probability of emission of a particle per unit time from a deformed axisymmetric elongated nucleus that rotates around its short axis. The emission process is subdivided into three stages: formation of the prefission configuration, emission of a particle from the nucleus, and motion of the particle to the detector.

If we consider a small section of surface with coordinate $\mathbf{r}$, area $d^2A$, and outer unit normal $\mathbf{N}$, then we can readily see that during a unit interval of time it can be intersected by a particle separated from it by a distance less than $\mathbf{N}\cdot\mathbf{v}'$. Here, $\mathbf{v}' = \mathbf{v} - [\boldsymbol{\omega}_\perp \times \mathbf{r}]$ is the velocity of the particle relative to the emission point, $\mathbf{v}$ is the velocity of the particle in the laboratory system, $\boldsymbol{\omega}_\perp = \mathbf{I}/J_\perp$ is the angular velocity of the nucleus, and $J_\perp$ is the moment of inertia of the nucleus for rotation around the short axis.

Denoting by $f(\mathbf{r}, \mathbf{p})$ the probability for formation of the prefission configuration, and by $\mathbf{k}(\mathbf{r}, \mathbf{p})$ the asymptotic momentum of a particle that starts from the point $\mathbf{r}$ with momentum $\mathbf{p}$, we can represent the probability for emission of a particle per unit time by the formula[37,40]

$$R_\Phi(\varepsilon, \mathbf{l}, \mathbf{n}; E, \mathbf{I}) = \int d^2A \int d^3p\,\Theta(\mathbf{Nv}')\,\mathbf{Nv}' f(\mathbf{r}, \mathbf{p})\,\delta[\varepsilon - \mathbf{k}^2(\mathbf{r}, \mathbf{p})/2m]\,\delta(\mathbf{l} - \mathbf{r}\times\mathbf{p})\,\delta[\mathbf{n} - \hat{\mathbf{k}}(\mathbf{r}, \mathbf{p})], \tag{40}$$

where the integration is extended to the entire nuclear surface and the entire $\mathbf{p}$ space.

Equation (40) describes the emission from a rotating nucleus during a unit interval of time that is taken to be very short compared with the rotation period $2\pi/\omega_\perp$. The angle $\Phi$ defines the orientation of the symmetry axis $\boldsymbol{\nu}$ of the nucleus in the plane perpendicular to $\mathbf{I}$ at the time of emission of the particle.

At temperatures appreciably lower than the nucleon separation energy, it is possible to ignore the correlations of the nucleons in the emitted particle with the nucleons of the residual nucleus resulting from the Pauli principle, and to represent the function $f(\mathbf{r}, \mathbf{p})$ in the separable form

$$f(\mathbf{r}, \mathbf{p}) = [g/(2\pi)^3]\,\omega(q)/\omega_x(Q). \tag{41}$$

Using the conservation of the energy and the angular momentum, we can express the thermal energy $q$ of the daughter nucleus in the form

$$q = E - S - \frac{p^2}{2m} - U(\mathbf{r}) - U_{\mathrm{LD}} - \frac{(\mathbf{I}-\mathbf{r}\times\mathbf{p})^2}{2J_\perp} - \frac{[(\mathbf{I}-\mathbf{r}\times\mathbf{p})\,\boldsymbol{\nu}]^2}{2J_{\mathrm{eff}}}, \tag{42}$$

where $U(\mathbf{r})$ is the potential energy of the particle, $U_{\mathrm{LD}}$ is the deformation energy, $J_{\mathrm{eff}} = (J_\parallel^{-1} - J_\perp^{-1})^{-1}$ is the effective moment of inertia, and $J_\parallel$ is the moment of inertia for rotation around the $\boldsymbol{\nu}$ axis.

Bearing in mind that $\mathbf{I}\cdot\boldsymbol{\nu} = 0$ and omitting the terms quadratic in $\mathbf{r}\times\mathbf{p}$, we can simplify the relation (42). Substituting this simplified expression for $q$ in (41) and using the thermal approximation for $\omega(q)$, we obtain

$$f(\mathbf{r}, \mathbf{p}) = C_\perp \exp[-(\mathbf{p}^2/2m + U(\mathbf{r}) - \boldsymbol{\omega}_\perp[\mathbf{r}\times\mathbf{p}])/\tau], \tag{43}$$

where the coefficient $C_\perp$ has the form

$$C_\perp = \frac{g}{(2\pi)^3}\exp[(E - S - U_{\mathrm{LD}} - I^2/2J_\perp - q')/\tau] \times \omega(q')/\omega_x(Q). \tag{44}$$

In (43) we readily recognize the Maxwell–Boltzmann distribution in a coordinate system rotating with frequency $\boldsymbol{\omega}_\perp$. The temperature $\tau$ in this expression is the reciprocal logarithmic derivative of $\omega(q)$ at $q = q'$, where $q'$ is the thermal energy, near which the Taylor expansion for the entropy is made.

Equations (40) and (43), (44) can be readily generalized to a nucleus of arbitrary shape rotating around one of its principal axes with moment of inertia $J_{\mathrm{rig}}$. To this end, it is sufficient to replace $J_\perp$ in these equations by $J_{\mathrm{rig}}$, and $\boldsymbol{\omega}_\perp$ by the corresponding angular velocity $\boldsymbol{\omega}_{\mathrm{rig}} = \mathbf{I}/J_{\mathrm{rig}}$.

### Small deformations

For spherical nuclei, the expression (40) must go over into (6). To see that this is indeed the case, we note first that for a spherical nucleus the last $\delta$ function in (40) can be expressed in the expanded form

$$\delta[\mathbf{n} - \hat{\mathbf{k}}(\mathbf{r}, \mathbf{p})] = (\mathbf{n}\hat{\mathbf{r}})\,\delta(\mathbf{n}[\hat{\mathbf{l}}\times\hat{\mathbf{r}}] - \cos\chi)\,\delta(\mathbf{n}\hat{\mathbf{l}}), \tag{45}$$

where

$$\hat{\mathbf{r}} = \mathbf{r}/r;\quad \hat{\mathbf{l}} = \mathbf{l}/l;\quad \cos\chi = \hat{\mathbf{k}}[\hat{\mathbf{l}}\times\hat{\mathbf{r}}].$$

When the variables $\mathbf{r}$ and $\mathbf{p}$ are replaced by $\mathbf{r}$, $\varepsilon$, and $\mathbf{l}$, the angle $\chi$ becomes a function of $\mathbf{r}$, $\varepsilon$, and $\mathbf{l}$. Therefore, $R_\Phi$ can be represented in the form

$$R = C\exp\left(-\frac{\varepsilon}{\tau} + \frac{\omega\mathbf{l}}{\tau}\right)\delta(\mathbf{n}\hat{\mathbf{l}}) \times \int d^2A\,(\mathbf{n}\hat{\mathbf{r}})\,\delta(\mathbf{n}[\hat{\mathbf{l}}\times\hat{\mathbf{r}}] - \cos\chi)\,g, \tag{46}$$

where we have used (43), omitted the index $\Phi$ in $R_\Phi$, and introduced the notation

$$g = \frac{1}{m}\int d^3p\,(\hat{\mathbf{r}}\mathbf{p})\,\Theta(\hat{\mathbf{r}}\mathbf{p})\,\delta\left(\varepsilon - \frac{p^2}{2m} - U\right)\delta(\mathbf{l} - \mathbf{r}\times\mathbf{p}). \tag{47}$$

It is convenient to perform the integration in (47) in a system in which the $z$ axis is directed along $\mathbf{r}$, and $\mathbf{l}$ lies in the plane $x0z$. As a result, we obtain

$$g = \frac{1}{r^2}\,\Theta\left(\varepsilon - U - \frac{l^2}{2mr^2}\right)\delta(\mathbf{l}\hat{\mathbf{r}}).$$

Substituting this expression in (46) we arrive at the relation

$$R = C\exp\left(-\frac{\varepsilon}{\tau} + \frac{\omega\mathbf{l}}{\tau}\right)\Theta\left(\varepsilon - U - \frac{l^2}{2mr^2}\right)\delta(\mathbf{nl})\,h, \tag{48}$$

where

$$h = \frac{1}{r^2}\int d^2A\,(\mathbf{n}\hat{\mathbf{r}})\,\delta(\hat{\mathbf{r}}[\mathbf{n}\times\hat{\mathbf{l}}] - \cos\chi)\,\delta(\hat{\mathbf{l}}\hat{\mathbf{r}}). \tag{49}$$

For a spherical nucleus, the function $\chi(\mathbf{r}, \varepsilon, \mathbf{l})$ depends only on $r$, $\varepsilon$, and $l$ and the integration in (49) over the surface of the sphere leads to $h = 1$. Identifying $r$ with $R_0$ and $U(r)$ with $E_0$, we find that (48) is identical to (6) without the term $-l^2/(2J\tau)$ in the argument of the exponential. As can

be seen from (24), for moderate spins this term can be ignored if $mR_0^2 \ll J$. This condition is satisfied for medium and heavy nuclei.

We note that the integral over $d^3p$ in (40) can be found analytically for a deformed nucleus as well if $\nu'\cdot\mathbf{N}\Theta(\nu'\cdot\mathbf{N})$ is replaced by $\nu\cdot\hat{\mathbf{r}}\Theta(\nu\cdot\hat{\mathbf{r}})$. As a result, the probability of decay per unit time is found to be proportional to the transmission coefficient, which depends on the Coulomb and centrifugal barriers at the emission point, the coordinates of which we recover from the given $\varepsilon$, $\mathbf{l}$, $\mathbf{n}$:

$$R_\Phi = C_\perp \exp\left(-\frac{\varepsilon}{\tau}+\frac{\omega l}{\tau}\right) \times \delta(\mathbf{nl})\left\{\Theta\left[\varepsilon - U(\mathbf{r}) - \frac{l^2}{2mr^2}\right]\right\}_{\mathbf{r}=\mathbf{r}(\varepsilon,\,\mathbf{l},\,\mathbf{n})}. \quad (50)$$

Analysis of the emission of particles from deformed nuclei based on such a "local" transmission coefficient was proposed in Refs. 9 and 26 and was later developed in Ref. 41. From the derivation of the expression (50) given above, it can be expected that this approach is valid for small deviations from a spherical shape, when $\mathbf{N} \simeq \hat{\mathbf{r}}$.

#### The functions $\rho_c(z)$ and k(r, p)

It follows from consideration of the limiting case of a spherical emitter that the surface over which the integration in (40) is performed must be identified with the surface of the potential barrier. For a spherical nucleus this is the surface on which $U(r)$ reaches a maximum. In this subsection, we extend this concept to the case of a deformed nucleus and describe the procedure for separating the function $\mathbf{k}(\mathbf{r}, \mathbf{p})$ (Refs. 42 and 43).

For an axisymmetric nucleus, it is convenient to describe the position of the particle in the rotating system by means of cylindrical coordinates $\rho$, $z$, $\varphi$. In these coordinates, the surface that defines the position of the potential barrier has the form $\rho = \rho_c(z)$, so that the problem reduces to expressing the function $\rho_c(z)$ in terms of the potential $U(\rho, z)$ of the particle.

A general picture of the nature of $U(\rho, z)$ is provided by the lines of force. We find the line of force $\rho(z)$ that passes through the point $(\rho_0, z_0)$ from the equation

$$d\rho/dz = U_\rho(\rho, z)/U_z(\rho, z), \quad (51)$$

where $U_\rho = \partial U/\partial\rho$, $U_z = \partial U/\partial z$, with the additional condition $\rho(z_0) = \rho_0$. For an elongated nucleus, the lines of force can be divided into two families: lines that remain in a restricted part of the $\rho z$ plane, and lines that recede to infinity. The lines of the two families tend asymptotically to the closed curve that separates the families and can be taken as $\rho_c(z)$.

To describe the rotation of the nucleus, we introduce the laboratory system 1, 2, 3 and the system $x, y, z$, which is rigidly attached to the nucleus. As is shown in Fig. 4, the $z$ axis is directed along the symmetry axis of the nucleus, and the $y$ and 3 axes coincide with $\mathbf{I}$. The coordinates of the particle in the rotating system $x, y, z$ can be expressed in terms of its laboratory coordinates $r_1, r_2, r_3$ by means of the formulas

$$x = -r_1\sin\Phi_t + r_2\cos\Phi_t, \quad y = r_3, \quad z = r_1\cos\Phi_t + r_2\sin\Phi_t, \quad (52)$$

where $\Phi_t = |\omega_\perp| t$ is the angle through which the nucleus turns during time $t$.

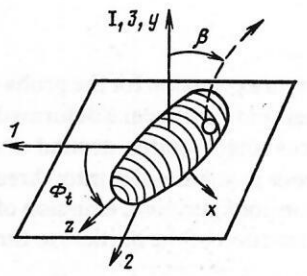


FIG. 4. Laboratory (1, 2, 3) and internal $(x, y, z)$ frames of reference and definitions of the angles $\beta$ and $\Phi_t$.

Since the particle is emitted from the surface of the potential barrier, its coordinates at the initial time satisfy the relations

$$r_1 = z, \quad r_2 = \rho_c(z)\cos\varphi, \quad r_3 = \rho_c(z)\sin\varphi, \quad (53)$$

which we shall write in the abbreviated form $\mathbf{r} = \mathbf{r}_c(z, \varphi)$.

To find the asymptotic properties of the particle for given $z$, $\varphi$, and $\nu'$, we initially go over from $z$, $\varphi$, $\mathbf{v}'$ to

$$\mathbf{r} = \mathbf{r}_c(z, \varphi) \text{ and } \mathbf{p} = m\mathbf{v}' + m[\omega_\perp \times \mathbf{r}], \quad (54)$$

and then solve Hamilton's equations for the functions $\mathbf{r}(t)$ and $\mathbf{p}(t)$:

$$\left.\begin{aligned} \dot{p}_1 &= (x/\rho)U_\rho\sin\Phi_t - U_z\cos\Phi_t, & \dot{r}_1 &= p_1/m;\\ \dot{p}_2 &= -(x/\rho)U_\rho\cos\Phi_t - U_z\sin\Phi_t, & \dot{r}_2 &= p_2/m;\\ \dot{p}_3 &= -(y/\rho)U_\rho, & \dot{r}_3 &= p_3/m, \end{aligned}\right\} \quad (55)$$

where $x$, $y$ and $\rho = (x^2+y^2)^{1/2}$, $z$ are expressed in terms of $r_1, r_2, r_3$ by means of (52).

Integrating the system (55) from $t = 0$ to $t = \infty$ with the initial condition $\mathbf{r}(0) = \mathbf{r}$, $\mathbf{p}(0) = \mathbf{p}$, we obtain the asymptotic momentum $\mathbf{k}(\mathbf{r}, \mathbf{p})$, and with it

$$\varepsilon = k^2/2m, \quad \cos\beta = \mathbf{kI}/(kI), \quad \gamma = \operatorname{arctg}(k_2/k_1), \quad (56)$$

where $\beta$ and $\gamma$ are the polar and azimuthal angles of the orientation of $\mathbf{n}$ in the system 1, 2, 3.

For a particle with charge $Z_p e$ moving in the Coulomb field of a spherical nucleus with charge $Z_d e$, there is a specific integral of the motion for this potential:[44]

$$\mathbf{A} = [\mathbf{p}\times\mathbf{l}] + c\hat{\mathbf{r}},$$

where $c = mZ_pZ_de^2$, $\hat{\mathbf{r}} = \mathbf{r}/r$. This can be used to find the explicit form of the corresponding function $\mathbf{k}(\mathbf{r}, \mathbf{p})$.

Taking into account the conservation of the vector $\mathbf{A}$, the orbital angular momentum $\mathbf{l}$, and the total energy of the particle, we can write down the relation

$$\mathbf{p}\times[\mathbf{r}\times\mathbf{p}] + c\hat{\mathbf{r}} = \mathbf{k}[\mathbf{r}\times\mathbf{p}] + c\hat{\mathbf{k}}, \quad (57)$$

where

$$\hat{\mathbf{k}} = \mathbf{k}/k; \quad k = (p^2 + 2mB)^{1/2}; \quad B = Z_pZ_de^2/r.$$

Solving Eq. (57) for $\mathbf{k}$, we obtain

$$\mathbf{k} = \frac{1}{\dfrac{m^2B^2}{p^2+2mB} + p_t^2}\left\{mB\left(\frac{p^2+mB}{(p^2+2mB)^{1/2}} - p_r\right)\hat{\mathbf{r}} + \left[p_t^2 + mB\left(1 - \frac{p_r}{(p^2+2mB)^{1/2}}\right)\right]\mathbf{p}\right\}, \quad (58)$$

where $p_r = \mathbf{p}\cdot\hat{\mathbf{r}}$, $p_t^2 = p^2 - p_r^2$.

It is sufficient to integrate the system (55) up to a time $t_f$ at which the nuclear forces and the nonspherical component of the Coulomb forces become negligibly small compared with the central Coulomb forces, after which, to obtain $\mathbf{k}$, we substitute the values of $\mathbf{r}(t_f)$ and $\mathbf{p}(t_f)$ in (58).

### Monte Carlo method

It is convenient to perform the integration in (40) by the Monte Carlo method. To this end, we divide the space ($\varepsilon$, $\cos\beta$, $\gamma$) into finite cells, which are labeled by indices $i, j, k$ and have sides $\Delta\varepsilon$, $\Delta\cos\beta$, $\Delta\gamma$, respectively. We obtain the probability $R_\Phi(i, j, k; \tau, I)$ for finding the particle in cell $i, j, k$ by integrating the expression (40) for $R_\Phi(\varepsilon, \mathbf{n}, \mathbf{l}; E, \mathbf{I})$ over $d^3l$ and over the volume $\Delta\varepsilon\Delta\cos\beta\Delta\gamma$ of this cell.

Going over from $\mathbf{v}$ to $\mathbf{v}'$ and noting that $\mathbf{N}d^2A = \mathbf{M}dzd\varphi$, where $\mathbf{M} = (\partial\mathbf{r}/\partial z)(\partial\mathbf{r}/\partial\varphi)$ is the outer normal to the surface at the point $\mathbf{r}$, we obtain

$$R_\Phi(i, j, k; \tau, I) = C_\perp m^3 \int\limits_{\substack{\varepsilon(z,\varphi,\mathbf{v}')\in i \\ \cos\beta(z,\varphi,\mathbf{v}')\in j \\ \gamma(z,\varphi,\mathbf{v}')\in k}} dz\, d\varphi\, d^3v' \mathbf{M}\mathbf{v}'\Theta(\mathbf{M}\mathbf{v}') \times \exp\left\{-\frac{mv'^2}{2\tau} - \frac{U(z)}{\tau} + \frac{m}{2\tau}\left[\boldsymbol{\omega}_\perp \times \mathbf{r}_c(z, \varphi)\right]^2\right\}. \quad (59)$$

It is here assumed that $\mathbf{M}$ is expressed by means of Eq. (53) in terms of $z$ and $\varphi$. For given $i, j, k$, the integration can be performed over $z$, $\varphi$, and $\mathbf{v}'$ for which $\varepsilon$, $\cos\beta$, and $\gamma$ are in the cell $i, j, k$.

Following the Monte Carlo method, we choose $z$ and $\varphi$ from a set of uniformly distributed random numbers, and $\mathbf{v}'$ from a set of random numbers distributed in accordance with the normal law. For given $z$, $\varphi$, and $\mathbf{v}'$ we first find $w$, which, by definition, is equal to the integrand in (59) divided by $\exp\{-mv'^2/2\tau\}$, and then, using Eqs. (54)–(56), we calculate $\varepsilon$, $\cos\beta$, and $\gamma$ for the cell in which the particle arrives, and we add $w$ to the probability so far accumulated for finding the particle in this cell. The calculations are repeated until the histograms of the angular and energy distributions are smooth.[37,45]

The total probability for emission of a particle per unit time (the width) $R(\tau, I)$ is equal to the sum of $R_\Phi(i, j, k; \tau, I)$ over $i, j, k$, i.e., to the right-hand side of (59) without the restrictions $\varepsilon\in i$, $\cos\beta\in j$, $\gamma\in k$. Integrating over $d^3v'$ and $d\varphi$ analytically, we obtain[40]

$$R(\tau, I) = 4\pi^2\tau^2 mC_\perp \int\limits_{-z_0}^{z_0} dz\, \rho_c \left(1 + \left(\frac{d\rho_c}{dz}\right)^2\right)^{\frac{1}{2}} \times \exp\left(-\frac{U(z)}{\tau} + \frac{m\omega_\perp^2}{2\tau}\left(z^2 + \frac{1}{2}\rho_c^2\right)\right) I_0\left(\frac{m\omega_\perp^2\rho_c^2}{4\tau}\right), \quad (60)$$

where $z_0$ is half the length of the nucleus, and $I_0(x)$ is a modified Bessel function. For a spherical nucleus, (60) goes over into (19) with $b_1 = 0$, $J_c = mR_0^2$, and $\beta_c = mR_0^2/J$.

At moderate temperatures, the nucleus makes many revolutions before it emits a particle, and the observed distributions are averaged over $\gamma$. The averaged distributions are described by the function $R(i, j; \tau, I)$, which is obtained from $R_\Phi(i, j, k; \tau, I)$ with $\Phi = 0$ by summation over $k$.

If the de-excitation process takes place as a chain of successive evaporations, equilibrium being established in the system after each of them, the angular and energy distributions of the particle $\nu$ are weighted means over the complete cascade:

$$\sigma_\nu^I(i, j) = \int d\tau\, \sigma_\nu^I(\tau) \frac{R(i, j; \tau, I)}{R(\tau, I)}, \quad (61)$$

where $\sigma_\nu^I(\tau)$ is the total cross section for the production of particle $\nu$ subject to the condition that the corresponding residual nucleus has temperature $\tau$. To calculate $\sigma_\nu^I(i,j)$, it is necessary to replace $w$ by the ratio $w/R(\tau, I)$ and introduce a random number that generates $\tau$ in accordance with the distribution $\sigma_\nu^I(\tau)$.

## 4. ELLIPSOIDAL SHAPES

### Trajectory function

We consider the properties of the functions $\rho_c(z)$ and $\mathbf{k}(\mathbf{r}, \mathbf{p})$ for a nucleus in the shape of an elongated ellipsoid of revolution. We denote by $a$ and $b$, respectively, the semimajor and semiminor axes of the mass distribution and introduce the ratio $\delta = b/a$. If $\delta$ is given, then $a = R_m/\delta^{2/3}$, $b = R_m\delta^{1/3}$, where $R_m = 1.225A_d^{1/3}$ is the radius of an equally large sphere,[46] and $A_d$ is the mass number of the daughter nucleus.

Following Ref. 47, we choose the nuclear potential in the form

$$U_n = -V_0\,[1 + \exp(l/a_0)]^{-1}, \quad (62)$$

where $V_0$ and $a_0$ are the depth and diffuseness of the potential,

$$l = \frac{1}{2}(a_n^4\rho^2 + b_n^4z^2)^{-1/2}(a_n^2\rho^2 + b_n^2z^2 - a_n^2b_n^2) \quad (63)$$

is the distance from the point $(\rho, z)$ to the contour on which $|U_n|$ is half its value at the center, $a_n = R_n/\delta^{2/3}$, $b_n = R_n\delta^{1/3}$, and $R_n$ is the radius of the potential.

We obtain the semimajor and semiminor axes of the ellipse that characterizes the charge distribution, $a_c$ and $b_c$, respectively, from the system of equations

$$a_cb_c^2 = R_c^3,\ a_c - a_n = b_c - b_n,$$

where $R_c = r_{0c}A_d^{1/3}$ is the radius of the charge distribution. By virtue of the second of these conditions, the gap between the charge distribution and the nuclear potential is approximately the same over the entire surface.

We calculate the Coulomb potential outside the uniformly charged elongated ellipsoid with semiaxes $b_c$, $b_c$, $a_c$ by analogy with the gravitational potential.[48] The result can be represented in the form

$$U_c = Q\left[\left(1 + \frac{1}{2}u - w\right)\ln(v_1 + v_2) + \frac{v_1w}{v_2} - \frac{1}{2}uv_1v_2\right], \quad (64)$$

where

$$Q = \frac{3}{2c}Z_pZ_de^2;\quad c = (a_c^2 - b_c^2)^{1/2};\quad u = \left(\frac{\rho}{c}\right)^2;\quad w = \left(\frac{z}{c}\right)^2;$$

$$v_1 = \left\{\frac{1}{2u}\left[(u + w - 1)^2 + 4u\right]^{1/2} - (u + w - 1)\right\}^{1/2};$$

$$v_2 = (1 + v_1^2)^{1/2}.$$

Figure 5 shows the lines of force of the potential $U = U_n + U_c$ in the exterior region and the line of the barrier $\rho_c(z)$ for the system $^{166}\mathrm{Er} + \alpha$ for $\delta = 1{:}2$. For the pa-

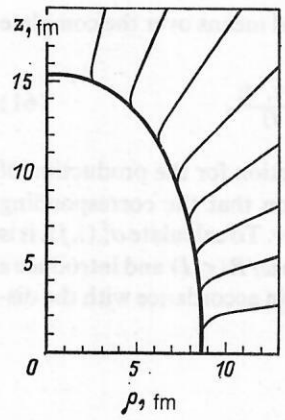


FIG. 5. Lines of force (thin curves) and line of the barrier (heavy curve) in the $^{166}Er + \alpha$ system for deformation 2:1.

rameters of the potential we have used the values $r_{0c} = 1.3$ fm, $V_0 = 50.2$ MeV, $R_n = (1.2A_d^{1/3} + 1.5)$ fm, and $a_0 = 0.564$ fm (Ref. 49). At large distances from the nucleus, the lines of force shown in the figure become radii drawn at angles 10,20,...,80° to the $z$ axis.

We determine the function $\tilde{\mathbf{k}}_c(\mathbf{r}, \mathbf{p})$ by substituting $U(z)$ in place of $B$ on the right-hand side of (58) for $\mathbf{k}(\mathbf{r}, \mathbf{p})$ calculated for a spherical Coulomb potential. An indication of the errors that arise when $\mathbf{k}(\mathbf{r}, \mathbf{p})$ is replaced by $\tilde{\mathbf{k}}_c(\mathbf{r}, \mathbf{p})$ is provided by Fig. 6, which shows the distribution functions $P(\Delta\varepsilon)$ and $P(\Delta \cos\beta)$ for the deviations $\Delta\varepsilon = \varepsilon - \tilde{\varepsilon}_c$ and $\Delta \cos\beta = \cos\beta - \cos\tilde{\beta}_c$, where

$$\tilde{\varepsilon}_c = \tilde{\mathbf{k}}_c^2/2m, \quad \cos\tilde{\beta}_c = \tilde{\mathbf{k}}_c\mathbf{I}/(\tilde{k}_c I).$$

The calculation was made for $I = 64$, $\tau = 1.8$ MeV, and $\delta = 1{:}2$. We generated $z$, $\varphi$, $\mathbf{v}'$ by means of a random-number generator: $\mathbf{v}'$ was distributed in accordance with a Gaussian law with zero mean and standard deviation $(\tau/m)^{1/2}$, $z$ and $\varphi$ were distributed uniformly, and the events were weighted with the weight function $w$.

It can be seen from Fig. 6 that $|\Delta\varepsilon| \lesssim 1$ MeV and $|\Delta\cos\beta| \lesssim 0.05$. Direct verification shows that $\tilde{k}_c^2 = \mathbf{p}^2 + 2mU(z)$ irrespective of the shape of $U(z)$, and, therefore, $\varepsilon_c$ is equal to the energy of the particle at the emission point. It follows from this that $\Delta\varepsilon$ characterizes the influence of the rotation of the residual nucleus on the energy of the emitted particle. We deduce from the figure that on the average $\varepsilon$ is smaller than $\varepsilon_c$. The lowering of $\varepsilon$ relative to $\varepsilon_c$ is particularly pronounced for particles with the lowest energies. This

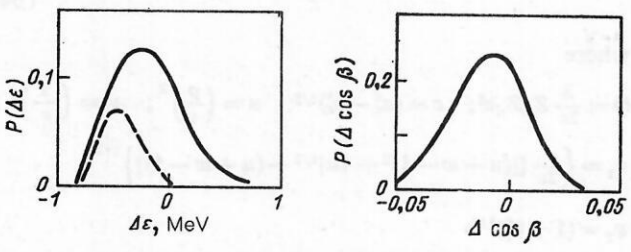


FIG. 6. Distribution functions $P(\Delta\varepsilon)$ (on the left) and $P(\Delta\cos\beta)$ (on the right) for $I = 64$, $\tau = 1.8$ MeV in the $^{166}Er + \alpha$ system. The broken curve is the distribution of the errors for $\varepsilon$ in the interval $(\varepsilon_{\min}, \varepsilon_{\min} + 5)$ MeV.

follows from the form of $p(\Delta\varepsilon)$ for particles with energies $\varepsilon$ in the range from $\varepsilon_{\min}$ to $\varepsilon_{\min} + 5$ MeV (broken curve in Fig. 6).

### Temperature distributions

It is convenient to calculate the evaporation cascades in the framework of the so-called $s$-wave approximation.[50] In it, the cross section for emission of particle $\nu$ from a nucleus with excitation energy $E$ and spin $I$ has the form

$$\left(\frac{d\sigma}{d\varepsilon}\right)_\nu = \sigma(E, I)\, g_\nu 2m\varepsilon\sigma_\nu(\varepsilon)\, \rho(E - S - \varepsilon, I)/D', \quad (65)$$

where

$$\sigma_\nu(\varepsilon) = \frac{\pi\hbar^2}{2m\varepsilon} \sum_l (2l+1)\, T_l^\nu(\varepsilon) \quad (66)$$

is the cross section for absorption of particle $\nu$ by the daughter nucleus, and $D'$ is the integral of the numerator over all particles and emission energies.

In the derivation of (65) from (35)–(37) the sum of $\rho(E - S - \varepsilon, j)$ over $j$ from $|I - l|$ to $|I + l|$ was replaced by $(2l + 1)\rho(E - S - \varepsilon, I)$. Using the temperature expansion for the level densities, one can show that such a replacement is justified when $(l\lambda)^2 \ll 1$, where $\lambda = \hbar\omega_{\text{rig}}/\tau$.

We calculate the cross sections $\sigma_\nu(\varepsilon)$ by means of the optical model, or we parametrize it. For example, substituting $T_l^{\text{erf}}(\varepsilon)$ in (66) and replacing the sum over $l$ by an integral, we obtain

$$\sigma^{\text{erf}}(\varepsilon;\, R_0,\, E_0,\, D_0) = \frac{\pi R_0^2 D_0}{\varepsilon\sqrt{2}} \left\{\frac{1}{\sqrt{\pi}} \exp(-\eta^2) + \eta(1 + \operatorname{erf}\eta)\right\}, \quad (67)$$

where

$$\eta = (\varepsilon - E_0)/D_0\sqrt{2}.$$

The relation (67) is analogous to the formula of Wong,[51] but it gives a more rapid decrease of the cross sections in the below-barrier region $\varepsilon < E_0$.

The level density of the deformed nucleus is

$$\rho(E, j) = (2j + 1)\, E_{j,\text{th}}^{-2} \exp[2(a_j E_{j,\text{th}})^{1/2}], \quad (68)$$

where the thermal energy of the nucleus is

$$E_{j,\text{th}} = E - \Delta - U_{\text{LD}} - j^2/2J_{\text{rig}},$$

the pairing correction $\Delta$ is equal to 0, $-11/\sqrt{A}$, and $-22/\sqrt{A}$ for even–even, even–odd, and odd–odd nuclei, respectively, and the level-density parameter is[52]

$$a_j = a\,(33 + 4\Delta_j^{-2/3} + 8\Delta_j^{1/3})/45,$$

where $\Delta_j = R_{\text{major}}/R_{\text{minor}}$ is the ratio of the largest and the smallest semiaxes of the nucleus.

The cross sections $\sigma_\nu^I(\tau)$ for decay of $^{90}Zr$ with $E_x = 142$ MeV and $I = 64$, corresponding to an elongated nucleus with $\delta = 0.5$, are shown in the upper part of Fig. 7. They were calculated by means of the statistical code ALICE[50] in a subprogram that calculates the cumulative energy spectrum of the particles. However, the contributions from the different steps of the evaporation cascade were sorted in accordance with the value of $\tau$, and not $\varepsilon$.

To take into account the influence of the deformation on $\sigma_\nu(\varepsilon)$, we replace $R_0$ and $E_0$ in (67) by $R(z)$ and $U(z)$

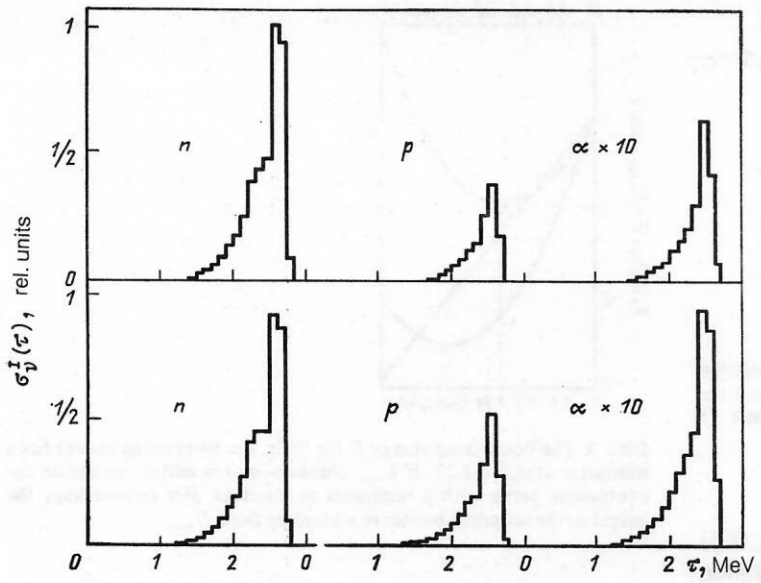


FIG. 7. Cross sections $\sigma_\nu^I(\tau)$ for decay of $^{90}$Zr with $E = 142$ MeV, $I = 64$, $\delta = 1/2$ for $\nu = n, p, \alpha$, calculated without allowance for deformation in the cross sections of the inverse processes (at the top) and with allowance for deformation in these cross sections (at the bottom).

and average over the surface of the nucleus:

$$\sigma_{\text{def}}(\varepsilon) = z_0^{-1}\int_0^{z_0} dz\,\sigma^{\text{erf}}(\varepsilon, R(z), U(z), D_0). \quad (69)$$

The calculation of $\sigma_\nu^I(\tau)$ with $\sigma_{\text{def}}(\varepsilon)$ is shown in the lower half of Fig. 7. The introduction of the deformation in $\sigma_\nu(\varepsilon)$ increased the yields of charged particles, but the shapes of the distributions with respect to $\tau$ were hardly changed.

For the calculation of $\sigma_{\text{def}}(\varepsilon)$, we took $\rho_c(z)$ to be an ellipse. In this case, the distance from the center to the surface is determined by the relation

$$R(z) = (R_0/\delta^{2/3})(\delta^2 + \sigma\xi^2(z/z_0)^2)^{1/2}, \quad (70)$$

where $\sigma = 1$ for a prolate and $\sigma = -1$ for an oblate (along the $z$ axis) nucleus, and

$$\xi = |(1-\delta^2)|^{1/2}, \quad \delta = \rho_0/z_0, \quad (71)$$

in which $\rho_0$ and $z_0$ are the semiaxes of the ellipse in the directions of the $\rho$ and $z$ axes. Note that $\delta < 1$ for $\sigma = 1$ and $\delta > 1$ for $\sigma = -1$. If $\delta$ is given, then $z_0 = R_0/\delta^{2/3}$.

As $U(z)$ we have taken the Coulomb energy $U_c(z)$ of a particle on the surface of a uniformly charged ellipsoid, which can be obtained from the expressions given in Ref. 48:

$$U_c(z) = E_0\delta^{2/3}(F - G(z/z_0)^2), \quad (72)$$

where

$$F = \frac{3}{4}(\sigma(K-1)/\xi^2 + K);$$
$$G = \frac{3}{4}(3\sigma(K-1)/\xi^2 - K);$$
$$K = \begin{cases} \frac{1}{2}\xi^{-1}\ln((1+\xi)/(1-\xi)) & \text{for } \sigma = 1, \\ \xi^{-1}\arcsin(\xi/(1+\xi^2)^{1/2}) & \text{for } \sigma = -1. \end{cases} \quad (73)$$

The parameters $E_0$, $R_0$, and $D_0$ for $\alpha$ particles and protons are obtained by fitting the cross section (67) to the optical cross section with initial values for $E_0$, $R_0$, and $D_0$ from Sec. 1. The deformation was not taken into account in the neutron cross sections.

**Angular anisotropy**

Experimental distributions $\sigma_\alpha^I(\varepsilon, \beta)$ for $\alpha$ particles from $^{110}$Sn(94 MeV), $^{114}$Sn(80 MeV), $^{138}$Nd(82 MeV), $^{164}$Yb(67 MeV), and $^{170}$Yb(135 MeV) (the excitation energy is given in the brackets) are given in Ref. 53. The magnitude and direction of **I** were found in each decay through detection of the cascade of $\gamma$ rays emitted by the residual nucleus. Fitting of the distributions $\sigma_\alpha^I(\varepsilon, \beta)$ to $A_0[1 + A_2^I p_2(\cos\beta)]$ yielded the coefficients $A_2^I$.

For emission of particles from a spherical nucleus, the angular anisotropy must decrease with decreasing $\varepsilon$, since the set of $l$ carried away by the particle becomes smaller. In the first three systems of those indicated above, $|A_2^I|$ decreases monotonically with decreasing $\varepsilon$. However, in $^{164}$Yb and $^{170}$Yb, $|A_2^I|$ begins to increase after the transition to the below-barrier region. Dilmanian *et al.*[54] attributed this anomaly to deformation of the nucleus. To test this suggestion, calculations of $A_2^I$ as a function of $\varepsilon$ were made in Ref. 55.

The trajectory function was taken to be $\tilde{\mathbf{k}}_c(\mathbf{r}, \mathbf{p})$. To imitate the diffused transmission coefficients, an average over the height of the barrier was taken by means of a normally distributed random number $X$ with zero mean and standard deviation $D_0$, which was added to $U_c(z)$ in the expressions for the weight function $w$ and for $\tilde{\mathbf{k}}_c(\mathbf{r}, \mathbf{p})$. For $R(\tau, I)$, the smoothing over the barrier height introduces a factor $\exp(\frac{1}{2}D_2^0/\tau^2)$ on the right-hand side of Eq. (60).

The averaging over $\tau$ was made with a weight function in the form of a triangle with base $(\tau_1, \tau_2) = (0.95, 2.3)$ MeV and (0.8, 1.4) MeV for $^{170}$Yb and $^{164}$Yb, respectively, which reproduce well the $\sigma_\alpha^I(\tau)$ calculated in accordance with the code of Ref. 50. For such distributions, $\tau = \tau_1 + (\tau_2 - \tau_1)\zeta^{1/2}$, where $\zeta$ is a random uniformly distributed number in the interval (0, 1).

There are appreciable uncertainties inherent in the procedure for measuring the angle of the emitted particle relative to the spin of the nucleus described in Ref. 53. The probability that measurement will yield for this angle the value $\beta$ under the condition that the true value is $\beta'$ is given by the response function $P(\beta, \beta')$ of the gamma spectrometer.[56]

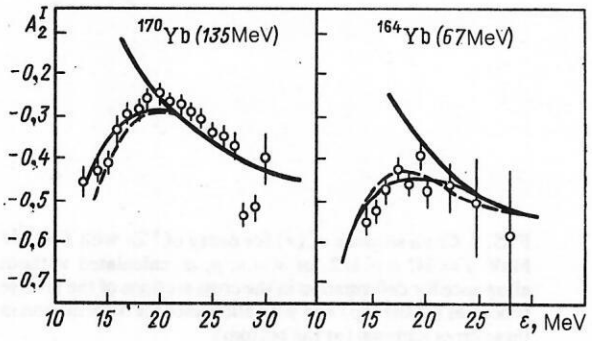


FIG. 8. Dependence of the coefficient $A_2^I$ on in the $\varepsilon$ in the case of emission of $\alpha$ particles from $^{170}$Yb and $^{164}$Yb for $I = 64$. The open circles are the experimental data of Ref. 53, and the curves are the calculation of Ref. 55 (see the text).

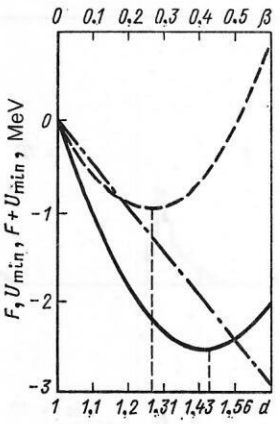


FIG. 9. The liquid-drop energy $F$ for $^{166}$Er, $I = 64$ (broken curve) has a minimum at $d_{eq} = 1.27$. If $U_{min}$ (broken line) is added, we obtain the continuous curve with a minimum at $d = 1.45$. For convenience, the height of the spherical barrier is subtracted from $U_{min}$.

We therefore averaged the theoretical cross sections $\sigma_\nu'(i,j)$ with the corresponding response matrix $P_{jj'}$, whose relation to $P(\beta, \beta')$ is given in Ref. 55.

Figure 8 shows the experimental and theoretical coefficients $A_2^I$ in the case $I = 64$ for $\alpha$ emission from $^{170}$Yb (135 MeV) and $^{164}$Yb (67 MeV) produced in the $^{20}$Ne + $^{150}$Nd fusion reaction at $E_{lab} = 177$ MeV and the $^{64}$Ni + $^{100}$Mo fusion reaction at 270 MeV, respectively. The calculations for a spherical nucleus (heavy curves) deviate sharply from the experimental data in the below-barrier region $\varepsilon < 17.5$ MeV. The calculation for a deformed nucleus with $d \equiv z_0/\rho_0 = 1.5$ (broken curve) reproduces the data in the complete range of $\varepsilon$.

The fit to the experimental data by a distribution from one decay with an effective $\tau$ is shown by the thin curves. The best agreement is obtained for $\tau = 1.8$ MeV, $d = 2.5$ ($^{170}$Yb) and $\tau = 1.2$ MeV, $d = 1.7$ ($^{164}$Yb). We see that the values of $d$ have been increased compared with their previous values. This increase is particularly large for $^{170}$Yb with its broad temperature distribution. The fact that the fitting of the cumulative spectrum by the spectrum of one decay can lead to unphysically large values of the deformation was first noted in Ref. 57.

### Fluctuation of the shape

It was found from study of $\gamma$ decay of giant dipole resonances in heated nuclei,[58–60] and also in theoretical calculations,[61,62] that for $^{166,160}$Er with $\tau = 1$–2 MeV and $I \sim 40$ the value of the equilibrium deformation $d_{eq}$ is close to 1.3. The excess of $d$ found above over $d_{eq}$ can be explained if one takes into account the statistical fluctuations of the shape of the nucleus and also the fact that the probability of $\alpha$ emission increases when the nucleus becomes more elongated.

The intensity of the population of the various shapes of the residual nucleus is given by the probability (60) of decay per unit time, regarded as a function of the deformation. It may be noted that the dependence of $R_\nu^I(\tau)$ on the shape is determined by two factors, namely,

$$R_\nu^I(\tau) \sim \exp\left(-(U_{LD} + I^2/2J_{rig})/\tau\right) \exp\left(-U_{min}/\tau\right), \quad (60a)$$

where $U_{min}$ is the minimal value of $U(z)$. The first factor occurs in $C_\perp$. The second factor approximately reproduces the dependence on the shape of the nucleus for the integral contained in (60).

The quantity $d_{eq}$ is defined as the $d$ for which

$$F = U_{LD} + I^2/2J_{rig}$$

attains a minimum. It follows from (60a) that for particle emission the preferred $d$ are those for which the sum of $F$ and $U_{min}$ is minimal. If $F$ depends smoothly on $d$ in the neighborhood of $d_{eq}$, then the addition of $U_{min}$, which decreases with $d$, can significantly shift the position of the minimum.

For the calculation of $F$, it is convenient to use the relations from Ref. 63:

$$U_{LD} = (16 \text{ MeV})\, A^{2/3}\left[\frac{2}{5}(1-x)\beta'^2 - \frac{4}{105}(1+2x)\beta'^3\cos 3\gamma\right];$$

$$J_{rig} = \frac{1}{5}Am_0(R_x^2 + R_z^2),$$

where

$$\beta' = \left(\frac{5}{4\pi}\right)^{1/2}\beta; \quad x = \frac{Z^2}{45A}; \quad \frac{\hbar^2}{2m_0} = 21 \text{ MeV·fm}.$$

Here, $\beta$ and $\gamma$ are the usual deformation parameters, related to the semiaxes of the nucleus by

$$R_x = R_0'\left(1 - \beta'\cos\left(\gamma - \frac{\pi}{3}\right)\right),$$

$$R_y = R_0'\left(1 - \beta'\cos\left(\gamma + \frac{\pi}{3}\right)\right),$$

$$R_z = R_0'(1 + \beta'\cos\gamma),$$

where

$$R_0' = r_0 A^{1/3}\left(1 - \frac{3}{4}\beta'^2 + \frac{1}{4}\beta'^3\cos 3\gamma\right)^{-1/3}.$$

Setting $\gamma = 0$, we found that $F$ for $^{166}$Er with $I = 64$ has a minimum at $d_{eq} = 1.27$ and that the addition of $U_{min}$ shifts the minimum to $d = 1.45$, a value that is close to the observed values (see Fig. 9). The suggestion that the thermal fluctuations in the shape of the nucleus could lead to a shift of the energy spectra of the charged particles to lower energies was made in Ref. 64.

## 5. TWO-PARTICLE CORRELATIONS

### Decay of a heated nucleus produced in a direct reaction

We consider a two-stage reaction $A(a, a'f)$; the nucleus $A$ is first excited as a result of inelastic scattering, and then fissions. It is assumed that the inelastic scattering is a direct

process and that the energy $E$ transmitted to the nucleus $A$ is so great that the nucleus arrives in a region with a high level density, for the description of which the statistical model is valid.

If the initial and final momenta of the particle ($\mathbf{k}_1$ and $\mathbf{k}_2$) are fixed, then the angular distribution of the fragments is described by the formula

$$W(\mathbf{n}_f; \mathbf{k}_2, \mathbf{k}_1) = C\int\limits_{(S)} d^2A\ (\mathbf{p}_1\mathbf{N})\ (R_f/R_{\text{tot}}) \times \exp\{-|[(\mathbf{p}_2 - \mathbf{p}_1) \times \mathbf{r}]\,\mathbf{n}_f|^2/2K_0^2\}. \quad (74)$$

We have used here the standard expression for the angular distribution of the fragments in the case of fission of a nucleus with given $\mathbf{I}$,[19,65]

$$W(\mathbf{n}_f; \mathbf{I}) = (R_f/R_{\text{tot}}) \exp[-(\mathbf{I}\mathbf{n}_f)^2/2K_0^2],$$

and $\mathbf{I}$ is identified with the angular momentum transferred to the nucleus by a particle that collides with it at the point $\mathbf{r}$.

The integration in (74) is over all points $\mathbf{r}$ of the nuclear surface at which the inelastic collision can occur. These points belong to the surface $S$ (see Fig. 10), which is the common part of the region 1 accessible for the incident particles and of the region 2, from which the particle can reach a detector without passing through the nucleus $A$ (Ref. 66). It is necessary to replace $I$ in the branching ratio $R_f/R_{\text{tot}}$ by $|(\mathbf{p}_2 - \mathbf{p}_1)\times\mathbf{r}|$, and to express $\mathbf{p}_2$ and $\mathbf{p}_1$ in terms of $\mathbf{r}$ and the corresponding $\mathbf{k}$.

For motion in a spherical Coulomb field, the functions $\mathbf{p}_1(\mathbf{r}, \mathbf{k}_1)$ and $\mathbf{p}_2(\mathbf{r}, \mathbf{k}_2)$ and the region $S$ can be found explicitly. Using the same approach that we used in Sec. 3 to obtain the function $\mathbf{k}(\mathbf{r}, \mathbf{p})$, we find

$$\mathbf{p}_1 = \frac{k_1}{(1-\hat{k}_{1r})\,\zeta_1 Q_1}\hat{\mathbf{r}} + \frac{1}{2}Q_1\mathbf{k}_1,$$
$$\mathbf{p}_2 = \frac{-k_2}{(1+\hat{k}_{2r})\,\zeta_2 Q_2}\hat{\mathbf{r}} + \frac{1}{2}Q_2\mathbf{k}_2, \quad (75)$$

Here

$$Q_1 = 1 + \sqrt{1 - \frac{2}{(1-\hat{k}_{1r})\,\zeta_1}},$$
$$Q_2 = 1 + \sqrt{1 - \frac{2}{(1+\hat{k}_{2r})\,\zeta_2}},$$
$$\hat{k}_{1r} = \hat{\mathbf{k}}_1\hat{\mathbf{r}}, \quad \zeta_1 = \varepsilon_1/E_{01}, \quad \hat{k}_{2r} = \hat{\mathbf{k}}_2\hat{\mathbf{r}}, \quad \zeta_2 = \varepsilon_2/E_{02},$$

where $\varepsilon_1$, $E_{01}$, $\varepsilon_2$, $E_{02}$ are the energy of the particle and the height of the Coulomb barrier in the entrance and exit channels. The sizes of the spots 1 and 2 are determined by the angles

$$\alpha_1 = \arccos[1/(2\zeta_1 - 1)], \quad \alpha_2 = \arccos[1/(2\zeta_2 - 1)], \quad (76)$$

which are swept out by the radius vector described from the center of the nucleus from the direction $-\mathbf{k}_1$ or $\mathbf{k}_2$ to the boundary of the corresponding spot.

If the energy of the incident particle satisfies $\varepsilon_1 \gg E, E_{01}$, then $\mathbf{p}_1 \simeq \mathbf{k}_1$, $\mathbf{p}_2 \simeq \mathbf{k}_2$, $k_2 \simeq k_1$, and $W(\mathbf{n}_f; \mathbf{k}_2, \mathbf{k}_1)$ can be found analytically.[67] In the quantum description of the direct process, these conditions correspond to the plane-wave approximation.

We denote by $W^{\text{in}}(\theta_r)$ the angular distribution of the fragments in the plane formed by the vectors $\mathbf{q} = \mathbf{k}_2 - \mathbf{k}_1$ and $\mathbf{k}_1$, and by $W^{\text{out}}(\phi_r)$ the angular distribution in the plane that passes through $\mathbf{q}$ and $\mathbf{k}_2 \times \mathbf{k}_1$, where $\theta_r$ and $\phi_r$ are measured from $\mathbf{q}$. Ignoring the dependence of $R_f/R_{\text{tot}}$ on $I$, we obtain, apart from a factor that does not depend on $\theta_r$ and $\phi_r$,

$$W^{\text{in}} = I_c(p^{\text{in}} \sin^2\theta_r); \quad (77)$$
$$W^{\text{out}} = I_c(p^{\text{out}} \sin^2\phi_r). \quad (78)$$

Here, $I_c(x)$ can be expressed in terms of the modified Bessel functions $I_0(x)$ and $I_1(x)$ by means of the relation

$$I_c(x) = \exp(-x)[I_0(x) + I_1(x)],$$

and the parameters $p^{\text{in}}$ and $p^{\text{out}}$ are determined by the kinematics of the direct reaction:

$$p^{\text{in}} = (k_1^2R_0^2/K_0^2)\sin^4(\theta/2); \quad (79)$$
$$p^{\text{out}} = (k_1^2R_0^2/K_0^2)\sin^4(\theta/2), \quad (80)$$

where $R_0$ is the radius of the nucleus, and $\theta$ is the scattering angle of the particle.

In Ref. 68, measurements of $W^{\text{in}}$ were made for the $(\alpha, \alpha' f)$ reaction on $^{232}$Th and $^{238}$U for $\varepsilon_1 = 120$ MeV, $\theta = 18°$, $E \simeq 6$ MeV, and $E \simeq 11$ MeV. The measured $W^{\text{in}}$, their fitting by means of (77), and the values of the fitting parameter $p^{\text{in}}$ are given in Fig. 11. The value of $K_0^2$ recovered by means of (79) from $p^{\text{in}}$ for $E = 9$–$13$ MeV is $K_0^2 \simeq 20$, and this is equal

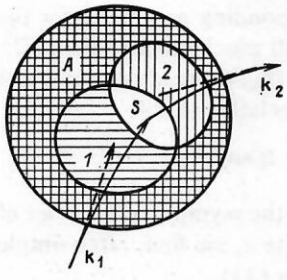


FIG. 10. Region of nuclear surface $S$ in which inelastic collision of the particle with the nucleus occurs. Because of the nuclear–Coulomb forces, the entry and exit trajectories (→) are deflected from the directions $\mathbf{k}_1$ and $\mathbf{k}_2$ (− →).

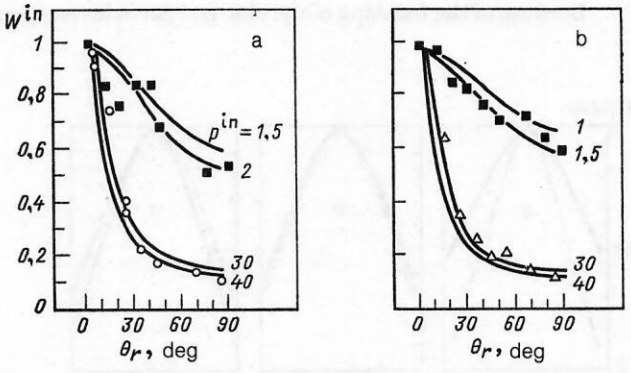


FIG. 11. Angular distributions of the fission fragments in the $(\alpha, \alpha' f)$ reaction on $^{232}$Th (a) and $^{238}$U (b) in the case of scattering of $\alpha$ particles with energy 120 MeV through 18° in the laboratory system (from Ref. 68) and their fitting in accordance with (77). The energy transferred is equal to 6.16–6.45 MeV (open circles), 9–13 MeV (black squares), and 5.85–6.15 MeV (open triangles).

to the $K_0^2$ obtained from the $^{235}U(n,f)$ reaction at excitation energy 10–12 MeV (Refs. 69 and 70).

### Decay of a heated nucleus produced in a deep inelastic reaction

To analyze the angular distributions of the particles evaporated from the heavy product of a deep inelastic reaction, the formula for the angular distribution $W(\cos\beta)$ of particles emitted from a nucleus with well-defined **I** is used. The direction of **I** is measured perpendicular to the plane of the deep inelastic reaction, and its value is identified with the mean spin of the heavy product.

For a spherical nucleus, we obtain $W(\cos\beta)$ from (26). Assuming (in accordance with the analogous assumption for a deformed nucleus) that $mR_0^2 \ll J$, we arrive at the expression (Refs. 15, 18, 25, and 26)

$$W(\cos\beta) = \exp(-b\cos^2\beta), \qquad (81)$$

where $b = (mR_0^2/2J^2\tau)I^2$. For a deformed nucleus, $W(\cos\beta)$ is proportional to the sum of $R(i,j;\tau,I)$ over $i$.

Stretching of the nucleus lowers the barrier at its ends, leading to enhanced emission of particles in the plane perpendicular to the spin, i.e., to a growth of the anisotropy. Simultaneously, because of the increase of $J_\perp$ there is a retardation of the rotation, and this reduces the anisotropy. It can be seen from Fig. 12 that at small spins and large deformations the first tendency is dominant, while at high spins these tendencies can compensate each other.

Hitherto, we have considered the case in which the time until emission of the particle, $t_\nu$, is much greater than the rotation period $T_\perp$ of the nucleus. In this case, the qualitative form of the angular distribution is the same for deformed and spherical nuclei. A different picture is observed in the opposite case of slow rotation, when $t_\nu \leqslant T_\perp/2$.

The angular distribution of the particles from a slowly rotating nucleus, $R(j,k;\tau,I)$, can be obtained from $R(i,j,k;\tau,I)$ by summation over the energy index. It can be seen from the example shown in Fig. 13 that at large deformations the emitted particles are focused in two peaks, which correspond to emission from the poles. Since the velocity of the tips of the nucleus is added to the velocity of the particles, the peaks are displaced relative to the points $(\cos\beta, \gamma) = (0,0), (0,\pi)$ that specify the orientation of the axis $\nu$ at the time of emission.

Because of the focusing of the charged particles emitted from the elongated nucleus, the two-particle correlation as a function of $\delta\gamma = \gamma_2 - \gamma_1$ must have a peak at the angle $\delta\gamma = \omega_\perp t_\nu$ through which the system turns between the two emissions. This can be used to extract $t_\nu$ from an experiment in the cases when $t_\nu$ lies between the time required for thermal equilibrium to be established (a few times $10^{-22}$ sec) and the rotation period of the nucleus.

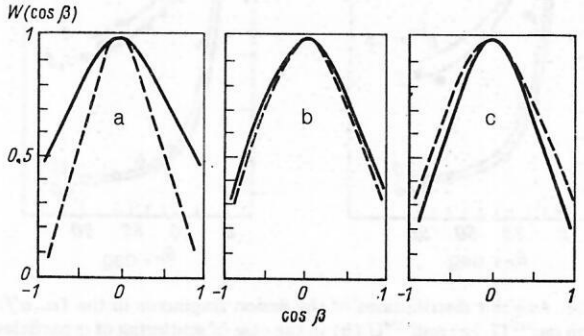


FIG. 12. The value of $W(\cos\beta)$ for $\alpha$ emission from a round (continuous curve) and elongated (with $\delta = 0.5$, broken curve) nucleus $^{143}$Gd. The calculations were made for the following cases: a) $I = 20$, $\tau = 1$ MeV; b) $I = 40$, $\tau = 2.5$ MeV; c) $I = 60$, $\tau = 4$ MeV.

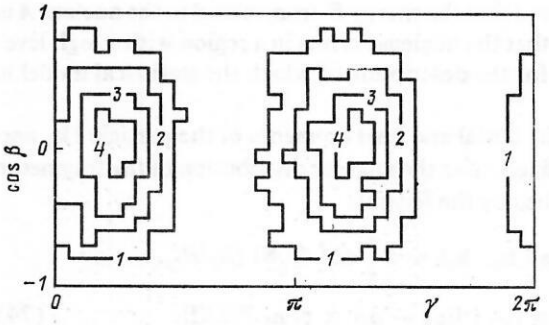


FIG. 13. Contour diagrams of the spatial distribution of $\alpha$ particles from $^{143}$Gd before averaging over $\gamma$. The calculation was made for $I = 45$, $\tau = 2.2$ MeV, $\delta = 0.5$ for $N = 10^5$ trials. The lines 1–4 correspond to 0.2, 0.4, 0.6, 0.8 of the maximal value.

### Particles accompanying a fusion–fission reaction

The formal analogy between the expression (26) for particle emission and the angular distribution of fission fragments makes it possible to apply the expression (33) for the two-particle correlation to the description of particle–fragment correlations. For this, it is sufficient to replace the parameter $\alpha_2$ in (33) by $1/(2K_0^2)$.

Compound nuclei detected in a counter after evaporation of several particles and $\gamma$ rays are called evaporation fragments. The upper limit of the region of decay by particle evaporation is denoted by $I_{ER}$. For $I \gtrsim I_{ER}$ and compound nuclei with $A = 100$–$200$ the dominant decay channel becomes fission. The dependence of $I_{ER}$ on $A$ is systematized in Ref. 71.

The values of $I$ near $I_{ER}$ contribute to the angular correlation of the particle $\nu$ and the fragment $f$. Because the particle is much lighter than the fragment, the ratio $R_f(E,I)/R_\nu(E,I)$ increases very rapidly with $I$. Therefore, the number of partial waves for which both evaporation and fission take place with significant probability will be small, and the right-hand side of (33) can be replaced by the integrand at the point $I_{ER}$.

As the estimates from Ref. 72 show, for $I = 50$–$100$ the parameter of the angular anisotropy of the fragments satisfies $CI^2 \geqslant 1$. Although the corresponding parameter for the particles, $BI^2$, is large,[73] it is still much smaller than $CI^2$. Therefore, for cases in which the fragments are detected not too near the beam the following relations hold:

$$CI^2 \sin^2\theta_f \gg 1, \quad C\sin^2\theta_f \gg B\sin^2\theta_\nu.$$

Using these inequalities and the asymptotic behavior of the Bessel function $I_0(x)$ at large $x$, we find, after simple transformations of the expression (33),

$$W(\mathbf{n}_\nu, \mathbf{n}_f) \sim \frac{1}{\sin\theta_f} W(\mathbf{n}_\nu; E, \mathbf{I}_{ER}), \quad \mathbf{I}_{ER} = \frac{[\mathbf{n}_b \times \mathbf{n}_f]}{\sin\theta_f} I_{ER}. \qquad (82)$$

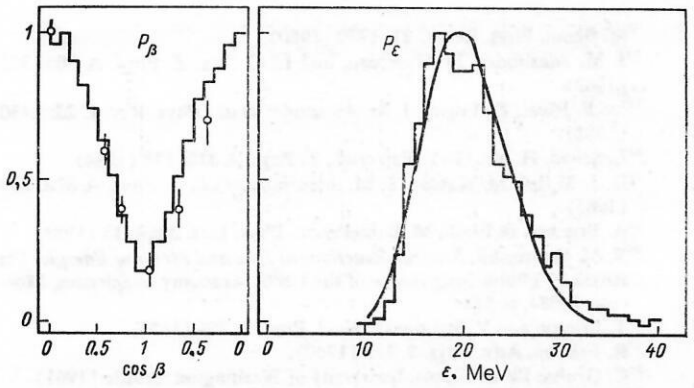


FIG. 14. Angular distributions of $P_\beta$ and the energy spectra $P_\varepsilon$ for $\alpha$ particles evaporated from $^{143}$Gd in coincidence with fission fragments. The histogram is the calculation for $\tau = 2.2$ MeV, $d = 2$, $I = 45$; the open circles and the continuous curve represent the experiment of Ref. 12.

where $\mathbf{n}_b$, $\mathbf{n}_\nu$, and $\mathbf{n}_f$ are unit vectors along the directions of the beam, particle, and fragment, respectively, and $W(\mathbf{n}; E, \mathbf{I})$ is defined in (26).

In accordance with (82), measurement of particles in coincidence with fission fragments (detected at fixed angle $\theta_f$ to the beam) makes it possible to study the emission of particles from a nucleus with spin $\mathbf{I}_{ER}$. As was shown in Ref. 45, this is also true for deformed nuclei. A numerical investigation of the accuracy of the relation (82) was made in Ref. 11.

In Ref. 12, a study was made of the emission of $\alpha$ particles in coincidence with fission fragments from the Cl + Ag reaction at energy 10 MeV per nucleon and for $\theta_f = 90°$. The energy spectra of the $\alpha$ particles measured at several angles were divided into three components in accordance with the three sources of the particles: the compound system and the two fragments.

In Fig. 14 we compare with calculations the angular and energy distributions ($P_\beta$ and $P_\varepsilon$, respectively) for $\alpha$ particles emitted from the compound system Gd; $P_\beta$ is measured in the plane perpendicular to $\mathbf{n}_f$, and $P_\varepsilon$ in the plane formed by $\mathbf{n}_f$ and $\mathbf{n}_b$. The optimal fit is obtained for $\tau = 2.2$ MeV, $d = 2$, $I \simeq 45$. According to Ref. 74, for nuclei near Gd and $\tau \simeq 2$ MeV the value of $I_{ER}$ is $\simeq 60$, i.e., appreciably higher than our value.

To estimate the possible influence of cascades on the parameters $I$ and $d$ deduced from experiment, we calculated $P_\varepsilon$ and $P_\beta$ with a triangle temperature distribution in the interval from 1 to 3.3 MeV. The value of $d$ did not change, but $I$ increased to 50.

### Two-particle decay of a heated nucleus produced in a fusion reaction

In this subsection, in which we consider the $^{108}$Ag($^{40}$Ar, $\alpha\alpha$) reaction at beam energy 285 MeV (Refs. 75 and 76), we investigate the behavior of the two-particle angular correlation in the case of decay of a compound nucleus produced in a fusion reaction. We assume that both particles are emitted at the beginning of the cascade, we take $\omega(q)$ from Sec. 1, and for $T_l(\varepsilon)$ we use the classical model with $E_0$ and $R_0$ (for $\alpha$ particles and protons) from the same subsection. For neutrons we set $E_0 = 0$, while we take $R_0$ to be the same as for protons.

Figure 15 shows the best fit of the angular correlations to the experimental points in a single plane [cases (a) and (b)] and in perpendicular planes [cases (c) and (d)]. It is obtained for $I_{max} = 90$. If it is assumed that the boundary between evaporation and fission is abrupt, $I_{max}$ can be identified with $I_{ER}$. The value of $I_{ER}$ extracted from the cross section for production of an evaporation fragment in the $^{40}$Ar + $^{108}$Ag reaction at 288 MeV is $I_{ER} = 80 \pm 7$ (Ref. 77).

The quantity $I_{ER}$ is often estimated as the $I$ at which the liquid-drop fission barrier[46] is equal to $S_n$. In the considered reaction, this gives $I_{ER} = 70$ (Refs. 78 and 79). For such an $I_{max}$, the angular correlations in a single plane are almost the same as for $I_{max} = 90$, while in perpendicular planes the anisotropy is almost halved (see Ref. 29).

It can be seen from this example that the angular correlations in perpendicular planes are very sensitive to $I_{ER}$. Nevertheless, it is not possible to deduce $I_{ER}$ unambiguously from just angular correlations, since the assumption that the $\alpha$ particles are evaporated at the beginning of the cascade is arbitrary, and with it the value of $\tau$. To take into account cascades, it is necessary to average the correlation function with a double temperature distribution for the daughter nuclei.

These calculations do not take into account the deformation of the compound nucleus, and this may also lead to errors. Such errors can be particularly large for small values of the parameter $b = \alpha I^2$. The case of small $b$, when the anisotropy is almost completely due to deformation, was considered in Ref. 80 for the example of the $^{32}$S($^{92}$Mo, $pp$) reaction at beam energy 86 MeV (c.m.s.).

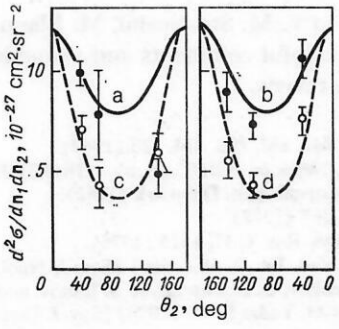


FIG. 15. Angular correlations in the center-of-mass system for two $\alpha$ particles in the case of $^{40}$Ar + $^{108}$Ar interaction at beam energy 285 MeV. The points are from the experiments of Refs. 75 and 76; the curves represent calculations in accordance with (33) for $I_{max} = 90$: a) $\theta_1 = 110°$, $\phi_1 = 0$, $\phi_2 = 0$; b) $\theta_1 = 110°$, $\phi_1 = 0$, $\phi_2 = 180°$; c) $\theta_1 = 110°$, $\phi_1 = 90°$, $\phi_2 = 0$; d) $\theta_1 = 110°$, $\phi_1 = 90°$, $\phi_2 = 180°$. The calculations are normalized to the data at the point $\theta_2 = 40°$ in case (a).

## CONCLUSIONS

In this paper, we have systematically presented the semiclassical theory of the emission of particles from spherical and deformed nuclei. In the case of spherical nuclei, we have given analytic expressions for the particle emission widths, the mean values of the energy and the angular momentum of the decay products, the angular distributions, and the two-particle correlations. The model contains a small number of parameters, which have a simple physical meaning and can be calculated by means of the optical model or found from fitting to experiments.

Besides the classical approximation for the coefficients of vector addition and the spherical functions, the model uses the thermal approximation for the level density, a 4-parameter approximation of the Laplace transforms for the transmission coefficients, and, in the case of the two-particle correlations, some other simplifications. Using numerical and analytical methods, we have studied the accuracy of these approximations and found that it is entirely adequate for the description of typical experiments.

In the case of deformed nuclei, we have given a closed expression for the probability of particle emission in the form of an integral of the probability current over the surface of the nucleus. We have shown that for small deformations it reproduces the expressions known from the literature. We have found equations for the position of the potential barrier and the approximate form of the trajectory function $\mathbf{k}(\mathbf{r}, \mathbf{p})$. We have obtained a simple expression for the width of particle emission from a deformed nucleus, and we have carried out a summation over cascades.

We have developed practical methods for calculating particle emission for nuclei of ellipsoidal shape. We have analyzed the experimental anisotropy of $\alpha$ particles with respect to the direction of the spin in the case of decay of excited Yb isotopes. If allowance is made for cascades and thermal fluctuations of the shapes, then the deformations of the daughter nuclei obtained from the fitting agree with independent data.

The advantages of the semiclassical model are particularly clearly revealed in the description of correlation experiments. In this paper we have given the semiclassical expressions for the particle–fragment, particle–heavy-ion, and particle–particle correlation functions and have considered applications of these expressions to analysis of the shape and spin of heated nuclei.

The author is grateful to V. M. Strutinskiĭ, M. Blann, and E. A. Cherepanov for helpful comments and valuable advice during writing of the review.

[1]J. R. Grover and J. Gilat, Phys. Rev. **157**, 802, 814, 823 (1967)
[2]J. D. Garrett and B. S. Nilsson, Notes on NBI Version of GROGI 2, Niels Bohr Institute, DK-2100, Copenhagen, Denmark (1982).
[3]F. Pühlhofer, Nucl. Phys. **A280**, 267 (1977).
[4]M. Beckerman and M. Blann, Phys. Rev. C **17**, 1615 (1978).
[5]A. S. Il'inov and V. D. Toneev, Yad. Fiz. **9**, 48 (1969) [Sov. J. Nucl. Phys. **9**, 30 (1969); V. S. Barashenkov, G. F. Zheregi, A. S. Il'inov, and V. D. Toneev, Fiz. Elem. Chastits At. Yadra **5**, 479 (1974) [Sov. J. Part. Nucl. **5**, 192 (1974)].
[6]A. S. Il'inov and E. A. Cherepanov, Preprint 37-84-68, JINR, Dubna (1984); A. S. Il'inov, Yu. Ts. Oganesyan, and E. A. Cherepanov, Yad. Fiz. **33**, 997 (1981) [Sov. J. Nucl. Phys. **33**, 526 (1981)].
[7]J. Gomes del Campo, R. G. Stockstad, J. A. Biggerstaff *et al.*, Phys. Rev. C **19**, 2170 (1979).
[8]N. N. Ajitanand, R. Lacey, G. F. Peaslee *et al.*, Nucl. Instrum. Methods **A243**, 111 (1986).
[9]M. Blann, Phys. Rev. C **21**, 1770 (1980).
[10]J. M. Alexander, D. Guerreau, and L. C. Vaz, Z. Phys. A **305**, 313 (1982).
[11]M. F. Rivet, D. Logan, J. M. Alexander *et al.*, Phys. Rev. C **25**, 2430 (1982).
[12]L. Schad, H. Ho, G.-Y. Fan *et al.*, Z. Phys. A **318**, 179 (1984).
[13]D. J. Moses, M. Kaplan, J. M. Alexander *et al.*, Z. Phys. A **320**, 229 (1985).
[14]A. Brucker, B. Lindl, M. Bantel *et al.*, Phys. Lett. **206B**, 13 (1988).
[15]V. M. Strutinskiĭ, *Nuclear Reactions at Low and Medium Energies* [in Russian] (Publishing House of the USSR Academy of Sciences, Moscow, 1958), p. 522.
[16]T. Ericson and V. Strutinsky, Nucl. Phys. **8**, 284 (1958).
[17]R. Ericson, Adv. Phys. **9**, 425 (1960).
[18]C. Gruhn, Ph.D. Thesis, University of Washington, Seattle (1961).
[19]V. M. Strutinskiĭ, Zh. Eksp. Teor. Fiz. **40**, 1794 (1961) [Sov. Phys. JETP **13**, 1261 (1961)].
[20]V. M. Strutinskiĭ, Yad. Fiz. 1, 588 (1965) [Sov. J. Nucl. Phys. **1**, 421 (1965)].
[21]T. D. Thomas, Nucl. Phys. **53**, 558 (1964).
[22]T. D. Thomas, Nucl. Phys. **53**, 577 (1964).
[23]D. C. Williams and T. D. Thomas, Nucl. Phys. **A92**, 1 (1967).
[24]D. W. Lang, Nucl. Phys. **77**, 545 (1966).
[25]T. Døssing, Nucl. Phys. **A357**, 488 (1981).
[26]T. Døssing, Ph.D. Thesis, NBI, Copenhagen (1978).
[27]M. A. McMahan and J. M. Alexander, Phys. Rev. C **21**, 1261 (1980).
[28]Tai Kuang-Hsi, T. Døssing, C. Gaarde, and J. S. Larsen, Nucl. Phys. **A316**, 189 (1979).
[29]V. P. Aleshin and S. R. Ofengenden, Izv. Akad. Nauk SSSR, Ser. Fiz. **50**, 982 (1986).
[30]L. C. Vaz, J. M. Alexander, and N. Carjan, Z. Phys. A **324**, 331 (1986).
[31]V. P. Aleshin and S. R. Ofengenden, Izv. Akad. Nauk SSSR, Ser. Fiz. **49**, 1003 (1985).
[32]V. P. Aleshin and S. R. Ofengenden, in *Proc. of the Sixth All-Union Conference on Neutrol Physics* (Kiev, 1983), Vol. 1 [in Russina] [TsNIIatominform, Moscow, 1984), p. 209.
[33]V. P. Aleshin and S. R. Ofengenden, J. Phys. G **11**, 243 (1985).
[34]K. A. Eberhard, P. von Brentano, M. Bönning, and R. O. Stephen, Nucl. Phys. **A125**, 673 (1969).
[35]D. L. Hill and J. A. Wheeler, Phys. Rev. **89**, 1102 (1953).
[36]P. J. Brussaard and H. A. Tolhoek, Physica **23**, 995 (1957).
[37]V. P. Aleshin, J. Phys. G **14**, 339 (1988).
[38]G. Szegö, *Orthogonal Polynomials* (American Mathematical Society, New York, 1959) [Russ. transl., Fizmatgiz, Moscow, 1962].
[39]S. Yu. Kun, S. M. Vydrug-Vlasenko, and V. Ph. Zavarzin, Z. Phys. A **325**, 213 (1986).
[40]V. P. Aleshin, Preprint KINR-86-13, Kiev (1986).
[41]N. N. Ajitanand, G. La Rana, R. Lacey *et al.*, Phys. Rev. C **34**, 877 (1986).
[42]V. P. Aleshin, Izv. Akad. Nauk SSSR, Ser. Fiz. **54**, 118 (1990).
[43]V. P. Aleshin, in *International Seminar School on Heavy-Ion Physics* (Dubna, 3–12 October 1989, D7-89-531) [in Russian] (JINR, Dubna, 1989), p. 137.
[44]L. D. Landau and E. M. Lifshitz, *Mechanics* (Pergamon Press, Oxford, 1960) [Russ. original, Fizmatgiz, Moscow, 1958], p. 53.
[45]V. P. Aleshin, Izv. Akad. Nauk SSSR, Ser. Fiz. **52**, 81 (1988).
[46]S. Cohen, F. Plasil, and W. J. Swiatecki, Ann. Phys. (N.Y.) **82**, 557 (1974).
[47]V. V. Pashkevich, Nucl. Phys. **A169**, 275 (1971).
[48]N. N. Lebedev, *Special Functions and Their Applications* (Prentice-Hall, Englewood Cliffs, N.J., 1965) [Russ. original, 2nd ed., Fizmatgiz, Moscow, 1963].
[49]G. R. Satchler, Nucl. Phys. **70**, 177 (1965).
[50]M. Blann and J. Bisplinghoff, Report No. UCID-19614.LLNL (1982).
[51]C. Y. Wong, Phys. Rev. Lett. **31**, 766 (1973).
[52]C. J. Bishop, I. Halpern, R. W. Shaw, Jr., and R. Vandenbosch, Nucl. Phys. **A198**, 161 (1972).
[53]N. G. Nicolis, D. G. Sarantites, L. A. Adler *et al.*, *The Variety of Nuclear Shapes* (World Scientific, Singapore, 1987), p. 526.
[54]F. A. Dilmanian, D. G. Sarantites, M. Jääskeläinen *et al.*, Phys. Rev. Lett. **49**, 1909 (1982).
[55]V. P. Aleshin, J. Phys. G **16**, 853 (1990).
[56]K. J. Honkanen, F. A. Dilmanian, D. G. Sarantites, and S. P. Sorensen, Nucl. Instrum. Methods Phys. Res. **A257**, 233 (1987).
[57]I. M. Govil J. R. Huizenga, W. U. Schröder, and J. Töke, Phys. Lett. **197B**, 515 (1987).
[58]J. J. Gaardhøje, C. Ellegaard, B. Herskind, and S. G. Steadman, Phys. Rev. Lett. **53**, 148 (1984).
[59]C. A. Gossett, K. A. Snover, J. A. Behr *et al.*, Phys. Rev. Lett. **54**, 1486

(1985).
[60]D. R. Chakrabarty, M. Thoennessen, S. Sen *et al.*, Phys. Rev. C **37**, 1437 (1988).
[61]P. Ring, L. M. Robledo, J. L. Egido, and M. Faber, Nucl. Phys. **A419**, 261 (1984).
[62]A. L. Goodman, Phys. Rev. C **37**, 2162 (1988).
[63]K. Neergård, V. V. Pashkevich, and S. Frauendorf, Nucl. Phys. **A262**, 61 (1976).
[64]U. Gollerthan, H. G. Clerc, E. Hanelt *et al.*, Phys. Lett. **201B**, 206 (1988).
[65]I. Halpern and V. M. Strutinski, in *Proc. of the Second United Nations Intern. Conf. on the Peaceful Uses of Atomic Energy* (Geneva, 1958), Vol. 15 (United Nations, Geneva, 1958), p. 408.
[66]K. L. Wolf, R. Vandenbosch, and W. D. Loveland, Phys. Rev. **170**, 1059 (1968).
[67]V. P. Aleshin, Yad. Fiz. **36**, 48 (1982) [Sov. J. Nucl. Phys. **36**, 28 (1982)].
[68]J. Van der Plicht, M. N. Harakeh, A. van der Woude *et al.*, Nucl. Phys. **A346**, 349 (1980).
[69]J. E. Simmons and R. L. Henkel, Phys. Rev. **120**, 198 (1960).
[70]R. B. Leachman and L. Blumberg, Phys. Rev. **137**, B814 (1965).
[71]S. M. Lee and T. Matsuse, J. Phys. Soc. Jpn. **54**, 272 (1985).
[72]B. B. Back and S. Bjørnholm, Nucl. Phys. **A302**, 343 (1978).
[73]M. Bantel, A. Brucker, H. Ho *et al.*, Jahresbericht, MPI für Kernphysik, Heidelberg (1984), p. 57.
[74]D. L. Hillis, J. D. Garrett, O. Christensen *et al.*, Nucl. Phys. **A325**, 216 (1979).
[75]A. G. Artyukh, V. V. Avdeĭchikov, G. F. Gridnev *et al.*, Yad. Fiz. **38**, 549 (1983) [Sov. J. Nucl. Phys. **38**, 326 (1983)].
[76]A. G. Artukh, G. F. Gridnev, M. Gruszecki *et al.*, Rev. Roum. Phys. **29**, 139 (1984).
[77]H. C. Britt, B. H. Erkkila, R. H. Stokes *et al.*, Phys. Rev. C **13**, 1483 (1976).
[78]M. Blann and T. A. Komoto, Phys. Rev. C **26**, 472 (1982).
[79]M. Blann, D. Akers, T. A. Komoto *et al.*, Phys. Rev. C **26**, 1471 (1982).
[80]R.-D. Ecker, J. Friese, H.-J. Körner *et al.*, Jahresbericht 1987, Beschleunigerlaboratorium der Universität und Technischen Universität, Munich (1987), p. 39.

Translated by Julian B. Barbour